# BIOSTRATIGRAPHICALLY CONSTRAINED AGES OF MISSISSIPPIAN MIXED CARBONATE-SILICICLASTIC SEQUENCES, STACK PLAY, ANADARKO BASIN, OKLAHOMA

By

BRANDON CHASE STUKEY

Bachelor of Science in Psychology

Oklahoma State University

Stillwater, Oklahoma

2006

Submitted to the Faculty of the
Graduate College of the
Oklahoma State University
in partial fulfillment of
the requirements for
the Degree of
MASTER OF SCIENCE
May, 2020

BIOSTRATIGRAPHICALLY CONSTRAINED AGES OF MISSISSIPPIAN MIXED CARBONATE-SILICICLASTIC SEQUENCES, STACK PLAY, ANADARKO BASIN, OKLAHOMA

Thesis Approved:

Jim Puckette

Thesis Adviser

Ashley Burkett

Cory J. Godwin

ACKNOWLEDGEMENTS

I would first like thank Dr. Jim Puckette for his guidance and encouragement throughout my graduate studies. His passion for teaching is undeniable and his commitment to continual learning is inspiring. I consider it a privilege to have studied under his direction.

I would also like to thank my committee members, Dr. Ashley Burkett and Dr. Cory Godwin for their support and thoughtful critiques of this thesis. A huge thanks goes out to Dr. Godwin for all his assistance, from teaching me how to pronounce the names of conodonts to providing SEM images and macrophotographs of specimens for use in this thesis. This study would not have been possible without his knowledge and expertise of Mississippian conodonts and his willingness to help.

Most of all, I want to thank my family. I don't believe I can adequately express in words my gratitude to my wife, Cianne, for her love and support throughout my studies. It has been a journey for sure, but she has been there every step of the way to lend an encouraging word when needed or sometimes a sterner "suggestion" to get back to work when motivation was lacking. I also want to recognize and thank my kids, Sutton and Tatum, for their unconditional love during this time. My hope is that I've, in some small way, instilled in them a sense of curiosity, continuous learning, and persistence.

Name: BRANDON STUKEY

Date of Degree: MAY, 2020

Title of Study: BIOSTRATIGRAPHICALLY CONSTRAINED AGES OF MISSISSIPPIAN MIXED CARBONATE-SILICICLASTIC SEQUENCES, STACK PLAY, ANADARKO BASIN, OKLAHOMA

Major Field: GEOLOGY

Abstract: The ages of Mississippian stratigraphic intervals within the STACK play of the Anadarko basin remain poorly understood due to the lack of biostratigraphic constraints. Godwin (2018) refined outcrop stratigraphy of Meramecian and Chesterian strata in northeastern Oklahoma and described siltstones and carbonates similar to those observed in STACK rocks. The four principal conodont biozones in the Meramecian through middle Chesterian outcrop sections were recognized in conodonts recovered from the Pan American, Barnes D-2 core from Major County. These results revealed that given the recovery of distinct taxa, these four key biozones are recognizable in a subsurface section and provide a mechanism for constraining the ages of the Mississippian intervals in the study area.

A sequence stratigraphic framework based on depositional facies and vertical stacking patterns within the Barnes core was correlated with the principal biozones and electrofacies from wireline logs. The contact between the Meramecian and Chesterian ages was identified honoring biostratigraphic constraints. The Osagean and Meramecian boundary however, could not be resolved due to limited conodont recovery. Osagean rocks may still be present in the Barnes D-2 core, in the approximately 200 feet of Mississippian carbonate section below the first identified biozone. Using stratigraphic surfaces including radiogenic intervals on the gamma-ray curve, wireline logs were correlated to identify clinoform geometry. Thirty (30) selected wireline logs were used to construct a cross section that illustrates the Mississippian stratigraphic architecture subparallel to paleodip. This cross section begins in Major County with the Pan American, Barnes D-2 in Section 23, T.22N., R.16W., and terminates with the Pan American, Effie B. York well in Section 13, T.18N., R.09W., northwestern Kingfisher County. This correlation shows that most of the Mississippian section in the Starr-Lacey field area, western Kingfisher County and eastern Blaine County, is early Chesterian and Meramecian.

TABLE OF CONTENTS

Chapter Page

LIST OF TABLES

Table Page

LIST OF FIGURES

Figure Page

Figure Page

# CHAPTER I

# INDTRODUCTION

## Summary of the Problem

The "Mississippian Limestone" is an informal term applied to the regionally extensive mixed carbonate-siliciclastic unconventional resource play spanning northwestern and north-central Oklahoma and southern Kansas. In the petroleum industry, the nomenclature of the Mississippian section in the STACK play, west of the Nemaha Ridge tends to be subdivided into stratigraphic intervals corresponding to North American regional age names (Chesterian, Meramecian, and Osagean). However, in this area, the Mississippian section has no formally established biostratigraphic framework or known chronostratigraphic markers and therefore lacks age constraint.

In November 2012, the Oklahoma State University (OSU)-Petroleum Industry Consortium *Reservoir Distribution and Characterization of Midcontinent Mississippian Carbonates* was formed, pairing faculty and students at Oklahoma State University with thirteen oil and gas companies in an effort to better understand the "Mississippian Limestone" in terms of its reservoir quality and distribution. Research conducted within the consortium was primarily focused on (1) describing the Mississippian lithostratigraphy, (2) developing sequence stratigraphic frameworks, and (3) constructing stratigraphic models to better understand the depositional architecture and improve

prediction of the distribution of reservoir facies across southern Kansas, northern Oklahoma, and the tristate region of Missouri, Arkansas, and Oklahoma (Bertalott, 2014; LeBlanc, 2014; Price, 2014; Childress, 2015; Doll, 2015; Flinton, 2016; Jaeckel, 2016; Shelley, 2016; Hunt, 2017).

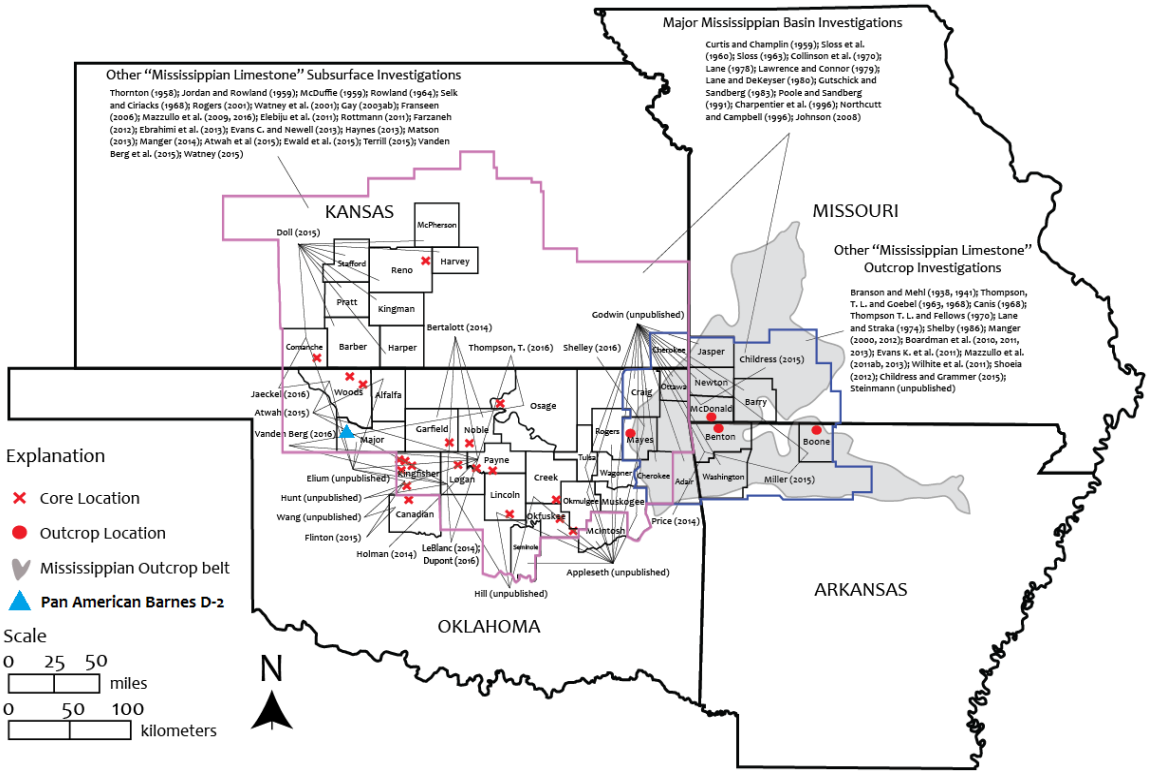


Figure 1. Map of Kansas, Oklahoma, Missouri, and Arkansas showing previous investigations into the "Mississippian Limestone" by researchers from the OSU-Petroleum Industry Mississippian Consortium and others outside of the consortium. Subsurface investigations are denoted by a red "X" marking core locations. Outcrop investigations are denoted by red dots within the gray infilled area showing the approximate boundary of the Mississippian outcrop belt. The approximate location for the Pan-American Barnes D-2 core used in this study is represented by the blue triangle. Modified from Hunt (2016).

The consortium's focus on sequence stratigraphy enhanced our understanding of the "Mississippian Limestone's" reservoir architecture and distribution. However, only a limited number of studies focused on correlating the sequence stratigraphic framework to the chronostratigraphic record. Three studies completed within the consortium's area of focus addressed temporal constraint of the Mississippian interval through conodont biostratigraphic analyses (Miller, 2015; Godwin 2017; Hunt, 2017) and one by means of chemostratigraphic concepts (Dupont, 2016). Two of these studies (Miller, 2015 & Godwin, 2017) primarily focused on outcrop conodont biostratigraphy in the tristate region of northeastern Oklahoma, northwestern Arkansas, and southwestern Missouri. Hunt (2017) used core-based conodont biostratigraphy to establish age-dates to the subsurface Mississippian interval across Logan, Payne, and Lincoln counties in north-central Oklahoma. As a result, biostratigraphic age-constraint within the subsurface Mississippian interval over the study area is geographically confined to east of the Nemaha Ridge.

Flinton (2016) defined the sequence stratigraphic hierarchy of the "Mississippian Limestone" in northwestern Kingfisher county, Oklahoma. Six lithofacies were identified and found to be consistent with a distally steepened carbonate ramp environment. The gross "Mississippian Limestone" in this area is interpreted to be a $2^{nd}$ order regressive pattern supersequence containing four, $3^{rd}$ order sequences that control the development and distribution of hydrocarbon reservoirs. It was also noted that reservoirs within this area are vertically compartmentalized by high-frequency Milankovitch band sequences ($4^{th}$ order) and cycles ($5^{th}$ order) which are thought to control distribution of individual flow units within reservoirs.

Jaeckel (2016) developed a sequence stratigraphic framework for the "Mississippian Limestone" in north-central Oklahoma and south-central Kansas, corresponding to a more proximal portion of the basin compared to Flinton (2016). The findings were consistent with previous regional descriptions, in that the identified lithofacies correspond to a distally steepened carbonate ramp environment. Similar to Flinton (2016), Jeackel (2016) found that the sequence stratigraphic hierarchy in the study area consisted of four, 3$^{rd}$ order sequences containing 4$^{th}$ order high-frequency sequences and 5$^{th}$ order high frequency cycles in an overall 2$^{nd}$ order regressive pattern supersequence. In both studies, 3$^{rd}$ order sequences were the primary control for correlative surfaces and sequence stratigraphic architecture. In both areas these 3$^{rd}$ order sequences are interpreted to be strike-elongate clinoforms that prograded basinward.

Dupont (2016) used carbon isotope data to construct chemostratigraphic curves for three cores across Logan and Payne counties in north-central Oklahoma. By comparing carbon isotope curves to those published for Mississippian intervals in select locations in the United States (Mii et al., 1999; Saltzman, 2002, 2003; Batt et al., 2007; Koch et al., 2014), attempts were made to assign age-dates to these intervals, albeit in the absence of biostratigraphic data.

Hunt (2017) used core-based conodont biostratigraphy to constrain the ages of "Mississippian Limestone" strata east of the Nemaha Ridge in Logan, Payne, and Lincoln counties in north-central Oklahoma. Using whole rock sampling and processing techniques, conodont elements were recovered from four cores and key taxa were identified. Based on prior relevant conodont studies (Collison et al., 1970; Dunn, 1970; Thompson and Fellows, 1970; Repetski and Henry, 1983; Baesemann and Lane, 1985;

Morrow and Webster, 1991; Krumhardt et al., 1996; Perri and Spaletta, 1998; Boardman et al., 2013; Bahrami et al., 2014; Miller, 2015; Godwin, 2017) these key taxa were shown to be relatively age diagnostic and important for defining age boundaries. Comparing his conodont biostratigraphic results to those of Dupont (2016), Hunt (2017) reinterpreted the chemostratigraphic record for the same three cores and found strong support for his hypothesis that Mississippian intervals in Logan, Payne, and Lincoln Counties of Oklahoma are Osagean to Chesterian in age.

Godwin (2018) refined outcrop stratigraphy of Meramecian and Chesterian strata in northeastern Oklahoma and identified four principal conodont biozones, providing a preliminary insight into the biostratigraphy of Mississippian intervals deposited within the Oklahoma basin. In addition to outcrop work, Godwin (2018) evaluated conodonts recovered in the 1960s from the Pan American Barnes Unit D-2 core in Major County, Oklahoma by the AMOCO Research Center in Tulsa. His evaluation revealed the same conodont biozones previously identified in the outcrop, providing a mechanism for constraining the ages of subsurface Mississippian intervals of the STACK play, Anadarko basin, Oklahoma.

## Problem Statement

To date, there are no formalized biostratigraphic results for age-dating Mississippian rocks in the Anadarko basin. Given the recognition of outcrop conodont biozones in the Pan-American Barnes D-2 core (Godwin 2018), an opportunity exists to temporally constrain ages of Mississippian intervals within the studied core through biostratigraphy. Using sequence stratigraphic concepts, these intervals can then be correlated with the framework developed by Flinton (2016) in a more distal portion of the basin.

### Purpose and Significance

The purpose of this study is to provide age-constraint through core-based conodont biostratigraphy to Mississippian strata within the northwest extension of the STACK play in Major County and subsequently to STACK play proper through sequence stratigraphic based wireline log correlation. The results of this study are most significant in that they (1) narrow the geological age range of Mississippian mixed carbonate-siliciclastic sequences prograding into the basin, allowing for more temporally accurate depositional models, (2) reveal relationships between biostratigraphically constrained intervals and observed high frequency ($4^{th}$ & $5^{th}$ order, respectively) sea-level cyclicity, and (3) provide an age-constrained locality within the STACK play to aid in correlating Mississippian strata in adjacent areas.

## Fundamental Questions

The fundamental questions to be addressed in this study are:

1. What is the geological age range of the Mississippian interval preserved in the Pan-American Barnes D-2 core in Major County, Oklahoma?
2. Is there a relationship between biostratigraphically constrained intervals and the high frequency sequences and cycles ($4^{th}$ and $5^{th}$ order, respectively) observed in the studies by Flinton (2016) and Jaeckel (2016)?
3. Can $3^{rd}$ order depositional sequences identified in the Barnes D-2 core, age-constrained by conodont biostratigraphy be correlated with deeper basinal settings and thus provide relative age constraint for Mississippian intervals within the STACK play in northwestern Kingfisher County, Oklahoma?

## Hypotheses and Objectives

The hypotheses for this study are that conodont biostratigraphy can be useful in constraining the age of the Mississippian interval preserved in the Pan-American Barnes D-2 core from Major County, Oklahoma and that this interval is Chesterian and Meramecian. Once the age of the Mississippian section in the Barnes D-2 core is established, subsequent sequence stratigraphic and core-based wireline log correlations can then be made basinward into deeper settings of the Anadarko basin and provide relative age constraint of Mississippian intervals within the STACK play and adjacent areas. The objectives of this study are to (1) establish a sequence stratigraphic framework based on depositional facies and vertical stacking patterns within the Pan-American Barnes D-2 core; (2) correlate the sequence stratigraphic framework to principal conodont biozones and electrofacies from wireline logs; and (3) illustrate the Mississippian stratigraphic architecture in the study area by construction of a wireline log cross section oriented subparallel to paleodip.

# CHAPTER II

## GEOLOGIC SETTING

The study area is located in northwestern Oklahoma in what is interpreted to be a transitional geological setting between the Anadarko shelf and basin. Bordering the study area are the Nemaha Uplift to the east, the Anadarko basin to the south and west, and the Anadarko shelf to the north. Figure 2 shows the location of this study's core in relation to major structural features of the Mid-Continent.

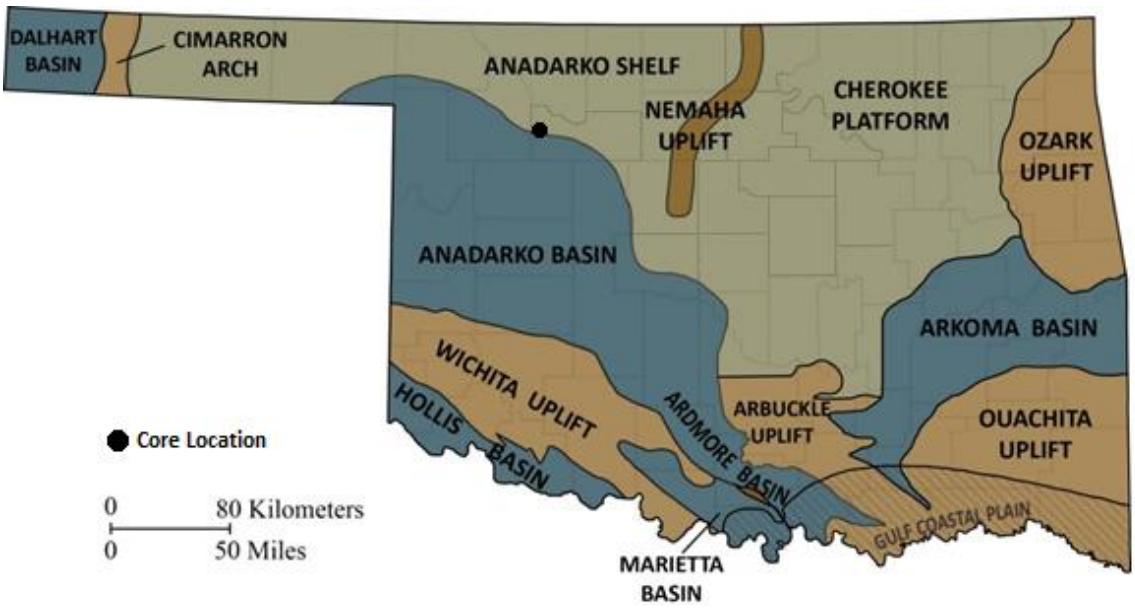


Figure 2. Map of Oklahoma illustrating major tectonic features. Areas shaded in blue represent basinal depressions relative to uplifted areas shaded in brown. The Anadarko shelf and Cherokee platform are shaded green. The approximate location of the Pan-American Barnes D-2 core used for this study is denoted by the black dot, west of the Nemaha Ridge. Modified from LeBlanc (2014) and Northcutt and Campbell (1996).

## Depositional Environment

The commonly accepted depositional model for Mississippian strata throughout the Mid-Continent is that of a carbonate ramp (Handford, 1995; Franseen, 2006; Mazzullo et al., 2009a). Carbonate ramps have low inclination slopes (typically less than 1°) and generally lack continuous reef trends, and can be further subdivided as homoclinal or distally-steepened based off of their profile. Distally-steepened ramps are differentiated from those with a homoclinal profile by a major break in slope occurring many kilometers seaward of high energy facies (Read, 1985). More recent OSU-Petroleum Industry Mississippian Consortium studies have revised the depositional model of the Mississippian strata of the Mid-Continent and proposed the more precise classification of a distally-steepened carbonate ramp. This revised model (Figure 3) was inferred from lithofacies, stacking patterns, and depositional geometries identified in core and wireline logs (LeBlanc, 2014; Price, 2014; Jaeckel, 2016). Observations supporting this revision include the strike-elongate clinoform geometry of interpreted 3rd order mixed carbonate-siliciclastic depositional sequences and the presence of mid-ramp debris flows identified in outcrop in southwestern Missouri (Childress, 2015).

## Paleogeography and Climate

Mississippian deposition, spanning from about 359 to 323 Ma (Gradstein et al., 2012), occurred throughout the Mid-Continent in a low latitude setting along the southern margin of a shallow and regionally extensive carbonate platform, known as the Burlington Shelf. A paleogeographic representation of the Mid-Continent depicting the

depositional setting during the late-early to middle Mississippian can be seen in Figure 4 (LeBlanc, 2014; Gutschick and Sanberg,1983; Lane and DeKeyser, 1980).

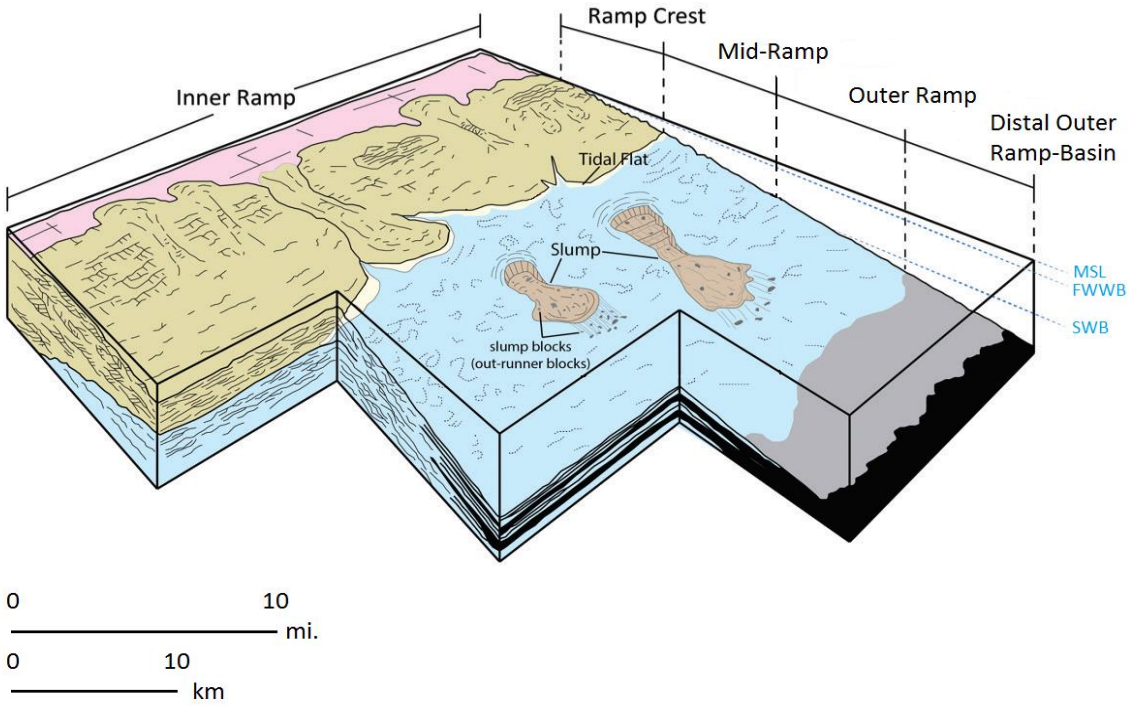


Figure 3. Schematic diagram illustrating a distally steepened carbonate ramp. Blue dotted lines represent approximate locations of mean sea level (MSL), fair weather wave-base (FWWB), and storm wave-base (SWB). Depositional facies in this study range from the relatively high energy environments of the distal ramp crest and lower mid-ramp to the lower energy environments of the distal outer ramp. Modified from Childress (2015) after Handford (1986).

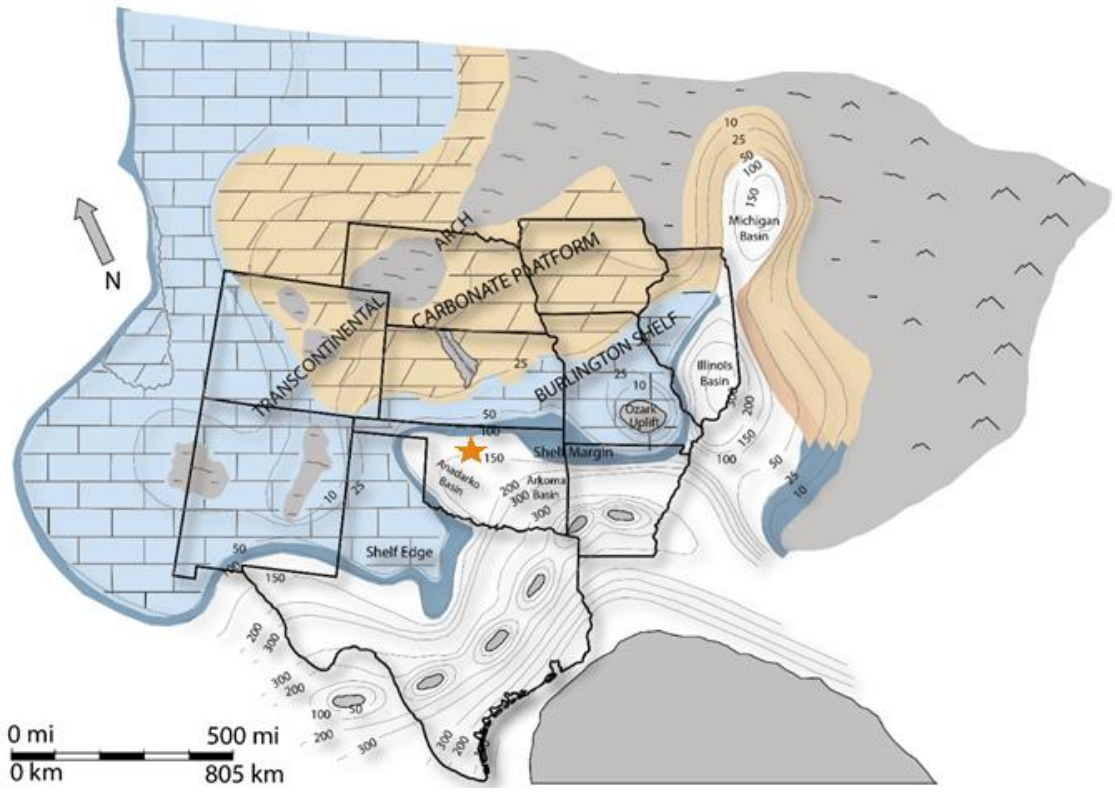


Figure 4. Regional paleogeographic time-slice map of the Early Mississippian, latest Tournaisian, middle Osagean. Study area is represented by the orange star. Map depicts areas of uplift (gray), limestone (light blue), dolomite (tan), fine-grained sediments (dark blue), and basin (white) facies. Estimated water depth represented by gray lines with a contour interval of 50 meters. Note the estimated water depth in the study area is approximately 140 meters. Modified from LeBlanc (2014) and Gutschick and Sandberg (1983).

Tropical to subtropical conditions existed throughout this region during the Early Mississippian (Curtis and Champlin, 1959; Gutschick and Sandberg, 1983; Franseen, 2006; Buggisch et al., 2008) with more arid and cooling conditions being established by the late Tournaisian (Early Mississippian) to early Visean (Middle Mississippian) and persisting through the Serpukhovian (Late Mississippian) (Franseen, 2006; Buggisch et al., 2008). The Mississippian Subperiod marks a transition between greenhouse climatic conditions of the Devonian and icehouse conditions of the Pennsylvanian (Read, 1995; Buggisch et al., 2008; Haq and Schutter, 2008). Analyses of carbon and oxygen isotopes in whole rock carbonates and conodont apatite, respectively, suggest a major cooling event and possible glaciation occurred towards the end of the Tournaisian and persisting into the Visean, and that a second glaciation event occurred during the Serpukhovian. Coinciding with these events, ocean surface temperatures fell from approximately 30°C during the Tournaisian to approximately 15°C during the Serpukhovian (Buggisch et al., 2008).

## Sea Level

Eustatic sea-level changes are primarily controlled by tectonics, ocean floor spreading, and global ice volume. Together, these mechanisms produce variations in sea-level know as sequences and cycles. Table 1 shows a hierarchy of cycles and sequences based on characteristics including duration, relative amplitude, relative sea-level rise/fall rate, and major processes responsible for each order of change. During greenhouse climatic conditions, as were present during the Devonian, sea-level fluctuations are often relatively small, generally less than 10 meters (Read and Horbury, 1993; Read, 1985). However, during icehouse conditions, such as in the Pennsylvanian, glaciation events

cause a gradual fall in sea-level proportional to the volume of continental ice. During deglaciations sea-levels rise rapidly, far exceeding most sedimentation rates, resulting in marine transgression. These relative sea-level fluctuations during icehouse conditions can be large, up to or exceeding 100 meters (e.g., Read and Horbury, 1993; Read, 1985).

Table 1. Sequence Stratigraphic Hierarchy Chart demonstrating the characteristics of 1st through 5th order cycles and their major controls responsible for sea-level fluctuations. Data compiled from Ross and Ross (1987a,b), Kerans and Tinker (1997), and Miall (2013). Redrafted by Hunt (2017) after Childress (2015).

| Sequence Stratigraphy Hierarchy Chart | | | | | |
|---|---|---|---|---|---|
| Tectono-Eustatic Cycle Order | Sequence Stratigraphic Unit | Duration (My) | Relative Sea Level Amplitude ft (m) | Relative Sea Level Rise/Fall Rate in/ky (cm/ky) | Major Control(s) on Sea Level Rise/Fall |
| First | Megasequence, or Supersequence Set, or Megacycle | 200 – 400 | n/a | <0.4 (< 1) | Tectonics (i.e., Wilson Cyclicity) |
| Second | Supersequence, or Supercycle | 10 – 100 | 164 – 328 (50 – 100) | 0.4 – 1 (1 – 3) | Tectonics, Ocean Floor Spreading, and Global Ice Volume |
| Third | Depositional Sequence, or Composite Sequence | 1 – 10 | 164 – 328 (50 – 100) | 0.4 – 4 (1 – 10) | Tectonics and Continental Ice Volume? |
| Fourth | High-frequency Sequence, Parasequence, or Cycle Set | 0.1 – 0.4 | 3 – 492 (1 – 150) | 16 – 197 (40 – 500) | Milankovitch Cyclicty (i.e., Eccentricity) |
| Fifth | High-frequency Cycle, or Parasequence | 0.02 – 0.04 | 3 – 492 (1 – 150) | 24 – 280 (60 – 700) | Milankovitch Cyclicty (i.e., Obliquity and Precession) |

## Mississippian Sea Level

As part of the Kaskaskia 1st order megasequence (Sloss, 1963), the Mississippian interval of the Mid-Continent is interpreted to be a 2nd order regressive supersequence (e.g., LeBlanc, 2014; Price, 2014; Jaeckel, 2016; Shelley, 2016; Godwin, 2017). As previously noted, the Mississippian represents a transition from the greenhouse climatic conditions of the Devonian to the icehouse conditions of the Pennsylvanian. Resulting from this transition, a long-term decline in sea-level began in the late Tournaisian, reaching a maximum highstand during the middle Osagean *anchoralis-latus* conodont zone (Gutschick and Sandberg, 1983), and terminated in the late Serpukhovian with a low near the Mississippian and Pennsylvanian boundary (Figure 5; Gutschick and Sandberg, 1983; Haq and Schutter, 2008). To help understand broad changes in depositional conditions of the Mid-Continent during the Mississippian, Figures 6 and 7 are Blakey (2018) paleogeographic representations of the Early to Middle Mississippian (~345 Ma) and Late Mississippian (~325 Ma), respectively.

In low inclination ramp environments (generally less than 1°), even minor sea-level fluctuations can have a profound effect on sediment deposition and shifts in facies (Burchette and Wright, 1992). During the Mississippian, sea-level fluctuations were generally large, up to and exceeding 100 meters (Read and Horbury, 1993). Given the low inclination of a distally steepened ramp, sea-level fluctuations at this scale can help explain the high degree of vertical and lateral heterogeneity of Mississippian lithofacies in the Mid-Continent.

Figure 5 shows the Mississippian coastal onlap and sea level curves. Of note in this figure is the decrease in duration of the short-term (3rd order) depositional sequences from the early Mississippian (approximately 3 m.y. in duration) to the middle to late Mississippian (approximately 1 m.y. in duration). Third-order depositional sequences in the Oklahoma basin during this time have been characterized by prograding carbonate-siliciclastic clinoforms (LeBlanc, 2014; Price, 2014; Doll, 2015; Flinton, 2016; Jaeckel, 2016) and are sometimes diachronous (Boardman et al., 2010, 2013; Miller, 2015; Godwin, 2017). Because conodonts are able to temporally resolve up to 3rd order sequences (Gradstein et al., 2012), or about one million years in Mississippian rocks in the Mid-Continent (Boardman et al., 2013; Godwin, 2017), this study aims to provide biostratigraphic age constraint for the mixed carbonate-siliciclastic sequences in the study area.

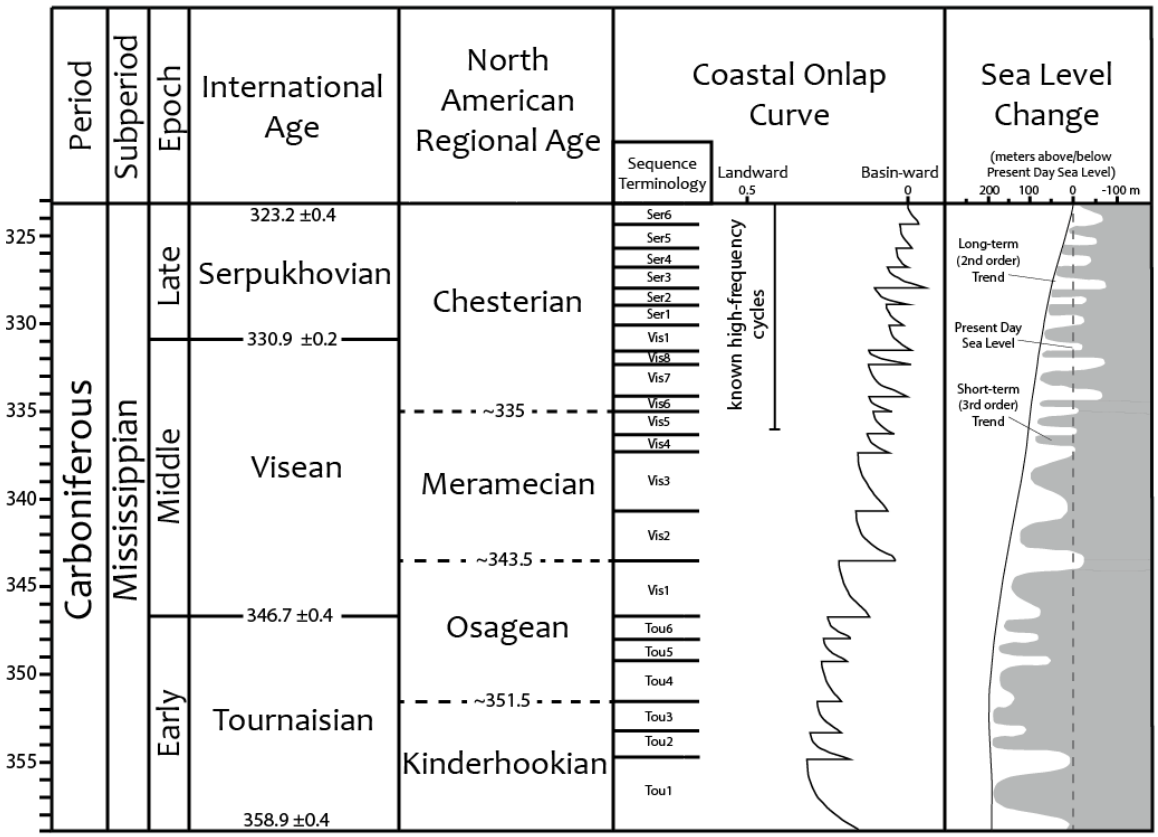


Figure 5. Mississippian Subperiod coastal onlap and sea level curves. Figure drafted by Hunt (2017) after Haq and Schutter (2008). Age-date data obtained from Gradstein et al. (2012). Coastal onlap sea-level change curves were modified by Hunt (2017) from Haq and Schutter (2008) to fit the geologic time scale updated by Gradstein et al. (2012). Sequence terminology obtained from Snedden and Liu (2010, 2011).

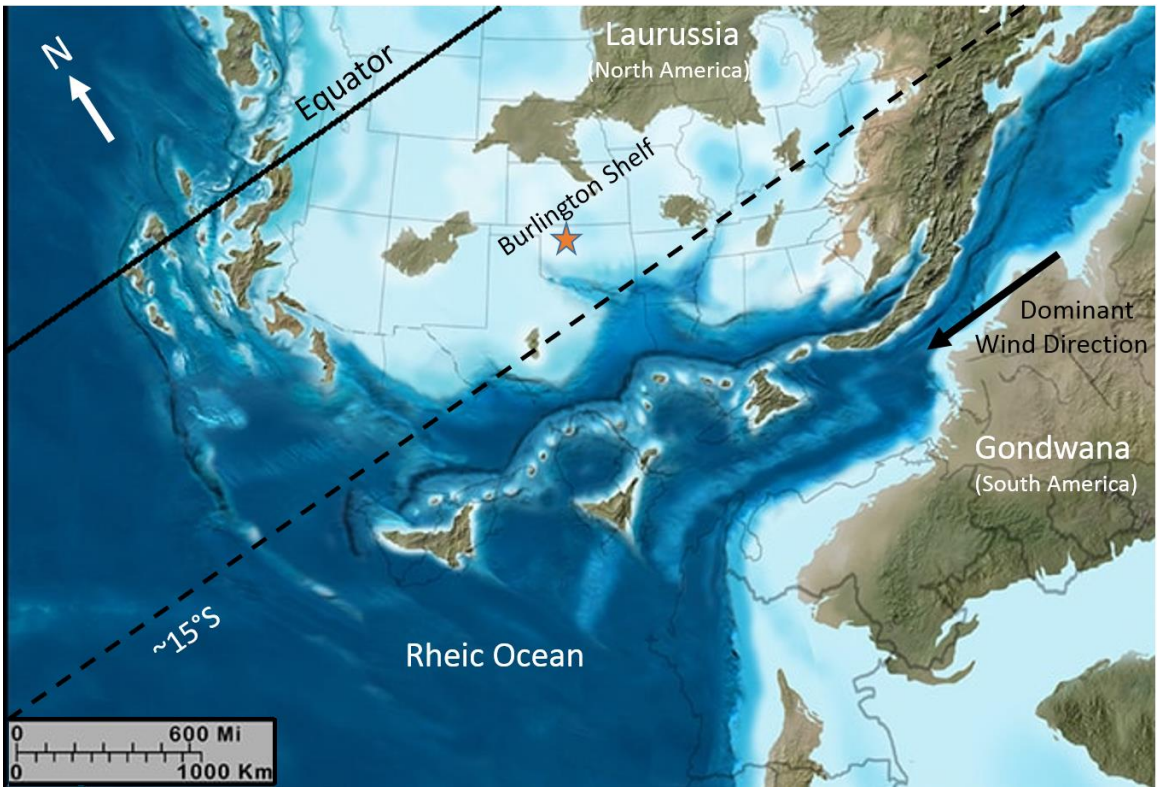


Figure 6. Early to Middle Mississippian (~345 Ma) paleogeographic time-slice map of ancestral North America. The study area, indicated by the orange star is located approximately 10°S of the paleoequator. The dominant wind direction is from present-day northeast. Land masses are indicated by brown and green colors. Relative water depth is indicated by the contrast of light blue (shallow water) and dark blue (deep water). Modified from Blakey (2018). Compare with Figure 7.

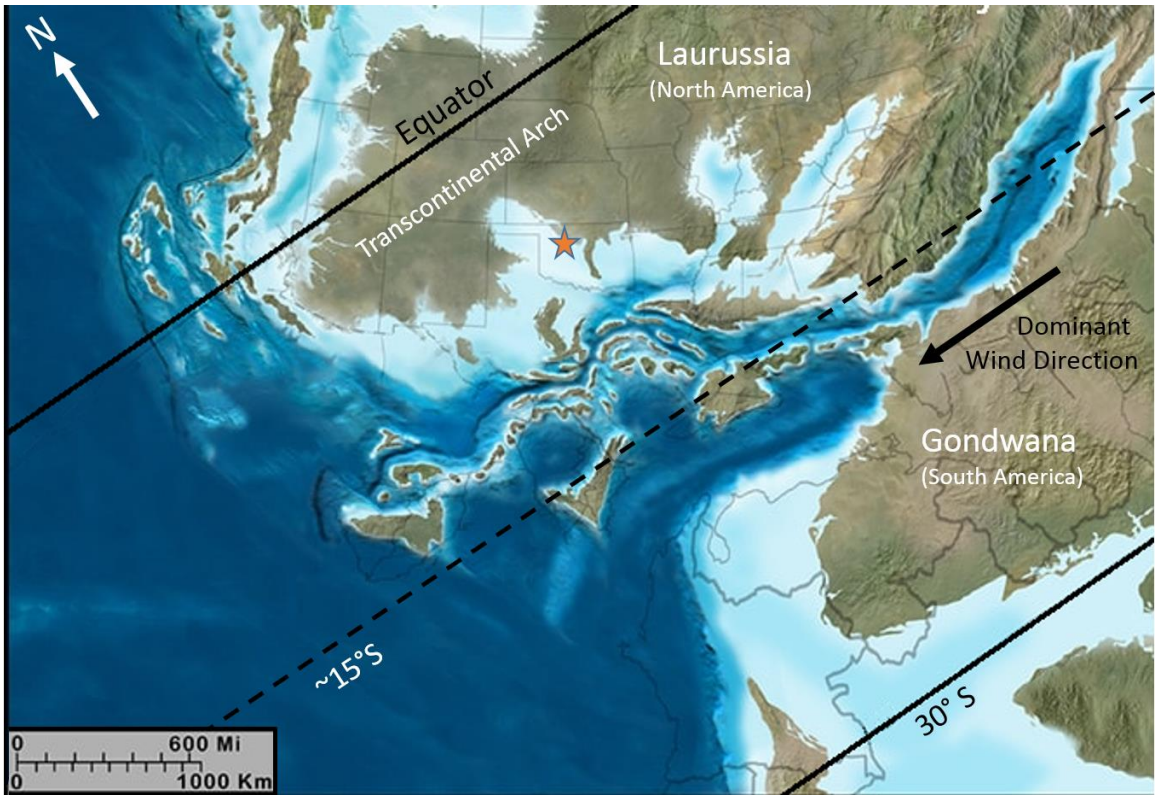


Figure 7. Late Mississippian (~325 Ma) paleogeographic time-slice map of ancestral North America. The study area, indicated by the orange star is located approximately 5°-10°S of the paleoequator. The dominant wind direction is from the present day northeast. Land masses are indicated by brown and green colors. Relative water depth is indicated by the contrast of light blue (shallow water) and dark blue (deep water). Modified from Blakey (2018). Compare with Figure 6.

## Regional Stratigraphy

The informally known “Mississippian Limestone” is a regionally extensive mixed carbonate-siliciclastic unconventional resource play spanning northwestern and north-central Oklahoma and southern Kansas. Prior research conducted in the laterally equivalent outcrop belt in northeastern Oklahoma, southwestern Missouri, and northwestern Arkansas established lithostratigraphic relationships and nomenclature. Generalized lithostratigraphic columns have been adopted for use by each state within the outcrop belt to correlate subsurface strata (Figure 8). Figure 8 highlights the variability in the lithostratigraphic nomenclature from state to state, making apparent how this can hinder correlations in an already stratigraphically complex system with time transgressive facies (Childress and Grammer, 2015; Miller, 2015).

Outcrop investigations of the Mississippian (Boardman et al., 2010; Mazzullo et al., 2011a,b & 2013) provided a more coherent and consistent lithostratigraphic framework and led to proposed modifications to the Mississippian nomenclature (Figure 9). These proposed modifications serve to standardize the nomenclature and improve lithostratigraphic characterization and subsurface correlations (Mazzullo et al., 2013). Although disagreements exist in the application of some of the terminology, it will be referred to throughout this study.

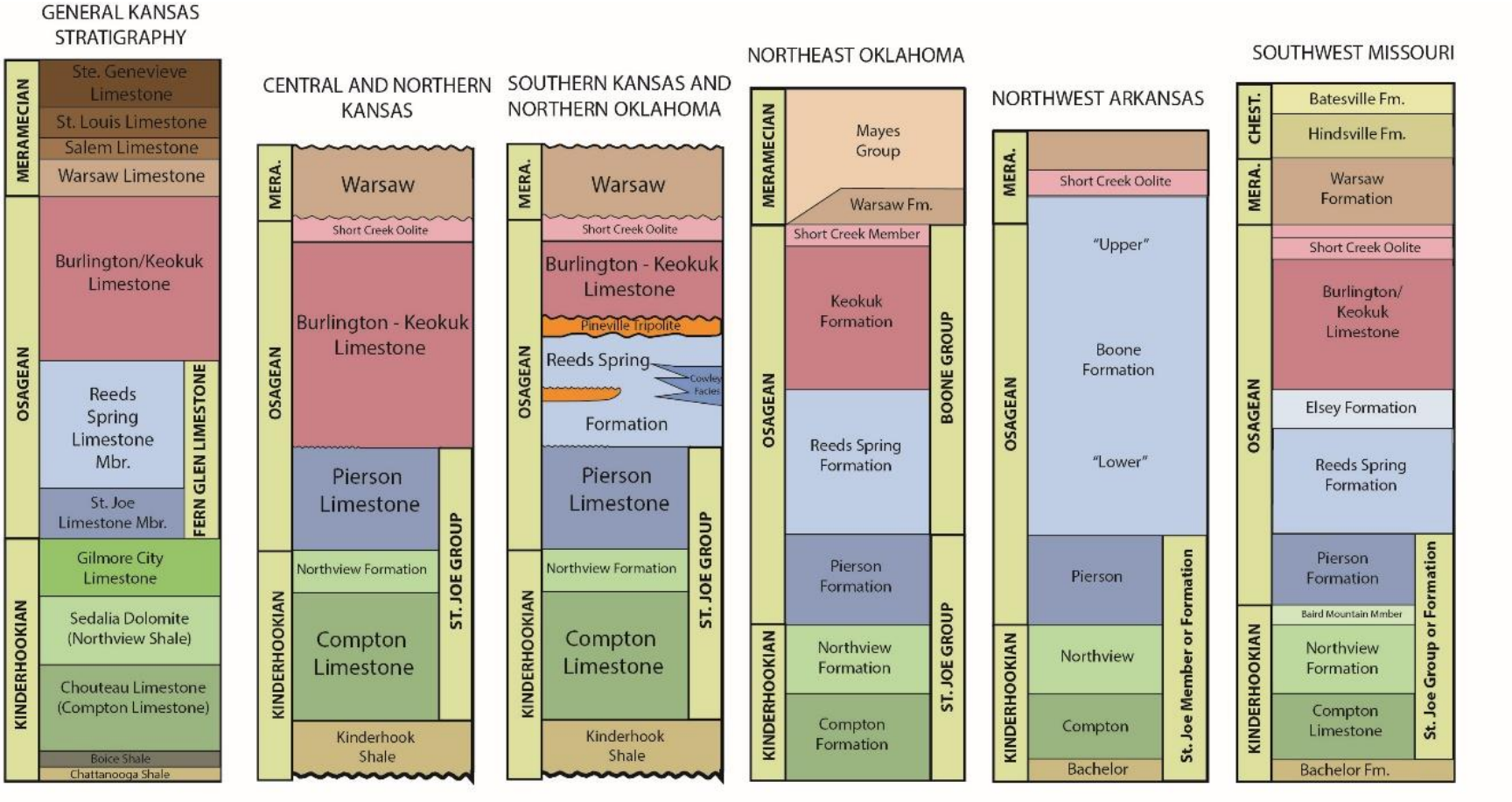


Figure 8. Regional stratigraphic columns of the Mississippian outcrop belt area. This figure highlights the variability in lithostratigraphic nomenclature of the Mississippian system from state to state in the Mid-Continent. Figure reproduced from Jaeckel (2016) after Mazzullo et al. (2011b, 2013) and Zeller (1968).

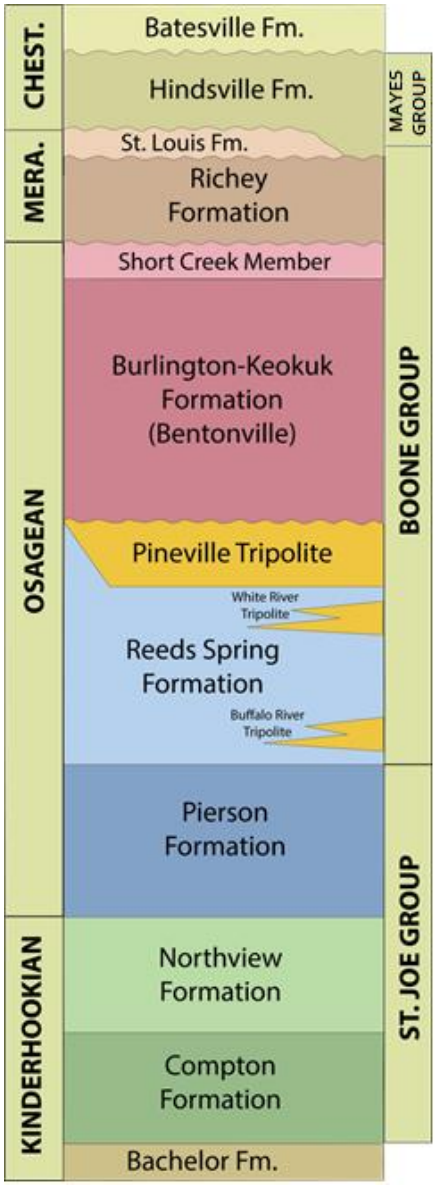


Figure 9. Stratigraphic column of the Mississippian Subsystem used for this study. Modified from Mazzullo et al. (2013).

It is important to note that Mississippian strata west of the Nemaha Ridge up to this point lack chronostratigraphic markers and thus, temporal constraint relies heavily on sequence stratigraphic concepts that do not directly relate to the chronostratigraphic record. Conodont biostratigraphic research (Thompson and Fellows, 1970; Boardman et al., 2013; Miller, 2015; Godwin, 2017 and 2018) conducted in the Mississippian outcrop belt reveals the time-transgressive nature of Mississippian depositional facies. This means that a lithostratigraphic marker, commonly given a formation name based solely on its depositional fabric, does not indicate a specific moment of geological time, but rather a unique depositional environment deposited within a genetically and laterally related facies mosaic. Childress and Grammer (2015) and Jaeckel (2016) highlight the problems associated with applying formation names based on lithological character (Figure 10).

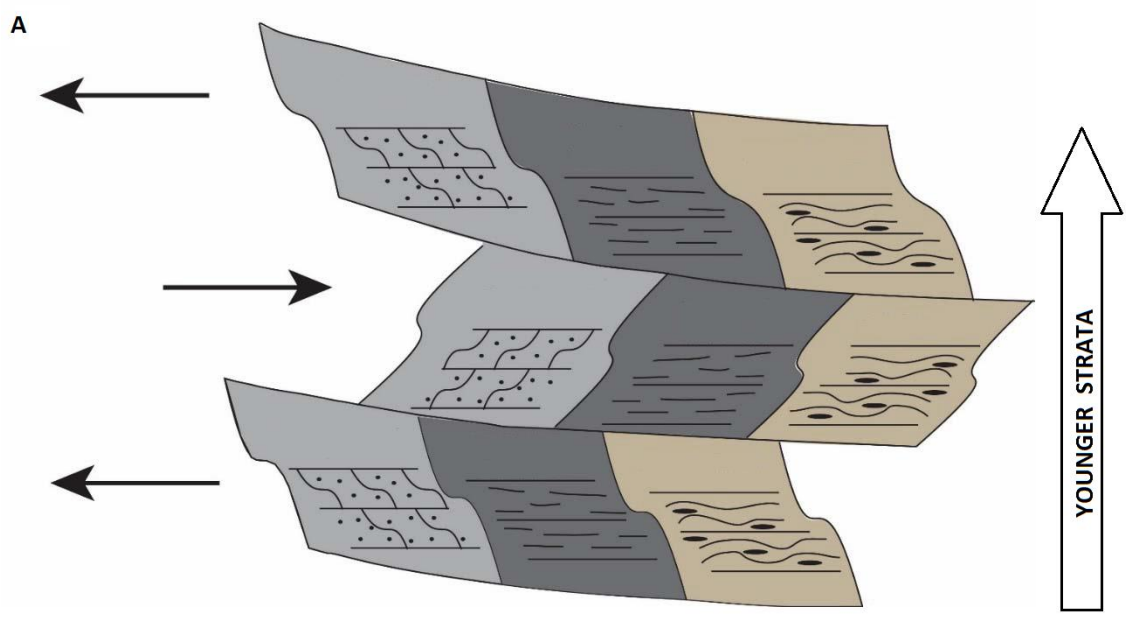

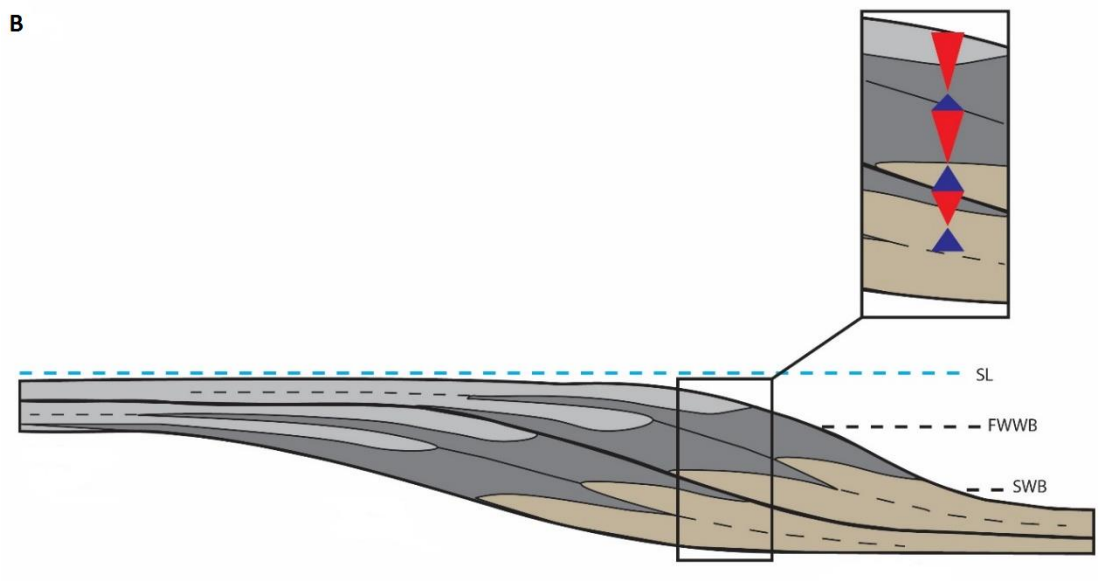


Figure 10. A) Conceptual diagram showing a range of facies deposited along a ramp setting with the more proximal portion to the left and distal portion to the right. The solid black arrows represent changes in base level resulting in lateral shifts of the three facies mosaics. The arrow to the right illustrates that younger strata or facies mosaics overlie older strata. This model helps illustrate the time-transgressive problem of applying formation names based on lithology alone. Modified from Jaeckel (2016) after Childress and Grammer (2015). B) A cross-sectional view of a distally-steepened ramp model illustrating how stacking patterns are formed by lateral shifts in facies as base level changes. Sequence boundaries are represented by thick black lines. Sea-level changes are represented by red (fall) and blue (rise) triangles. Modified from Jaeckel (2016).

Because there are no formal chronostratigraphic markers or an established biostratigraphic framework for the Mississippian interval west of the Nemaha Ridge, the petroleum industry has historically applied the informal term “Mississippian Limestone” to the gross interval. It is interpreted to be Mississippian in age based on regional-scale cross sections and correlations to nearby age-constrained Mississippian strata (e.g., Jordan and Rowland, 1959). There has also been a tendency to subdivide Mississippian

stratigraphic intervals based on log and/or core data and name them with terms corresponding to North American regional age names (Chesterian, Meramecian, and Osagean). However, as previously mentioned, the Mississippian section in this area has no formally established biostratigraphic framework or known chronostratigraphic markers, therefore these names may be applied erroneously, leading to further confusion regarding stratigraphic relationships. A biostratigraphic framework is needed to temporally constrain the Mississippian intervals in the study area to enhance stratigraphic correlations and better predict the distribution of oil and gas reservoir facies.

# CHAPTER III

# CONODONT BIOSTRATIGRAPHY

## Background

Conodonts have been used as biostratigraphic markers since the early twentieth century (Roundy, 1926). Seventy years prior, German paleontologist Christian Pander first discovered these teeth-like fossils and described conodont elements as "tiny, lustrous, elongated remains very similar in shape to fish teeth…" (translated by Sweet and Cooper, 2008 after Pander, 1856). Upon examination of his large collection of conodont elements, Pander noticed an absence of skeletal remains and concluded that it was highly unlikely that conodonts contained any other hard parts. He also noted similarities between the teeth of conodonts and modern-day hagfish and lampreys and suggested a possible relationship (Sweet and Cooper, 2008). Despite Pander's discovery, conodont elements were essentially regarded as paleontological curiosities and their value would lie largely dormant until a study by Ulrich and Bassler (1926) sparked interest in their biostratigraphic use in the United States (e.g., Roundy, 1926; Stauffer, 1930; Gunnell, 1931; Stauffer and Plummer 1932). Since then, conodonts have proven to be useful around the world as biostratigraphic markers for Middle Cambrian to Late Triassic age sedimentary rocks (Hunt, 2017). For a concise summary of the conodont animal and conodont elements, see chapter V. of Hunt (2017).

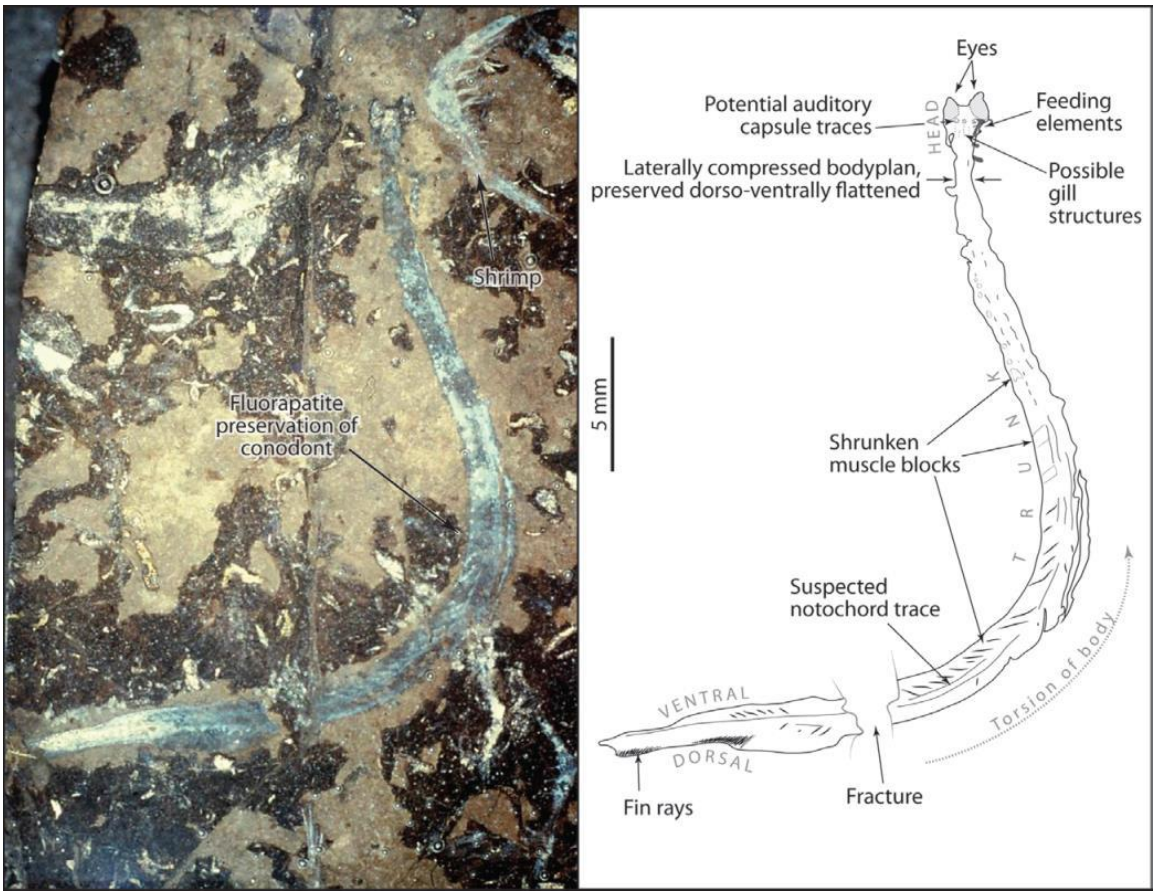


Figure 11. Conodont specimen in plan view. The photograph (left) shows a well preserved conodont specimen discovered in the Granton shrimp beds of Edinburgh, Scotland. Also pictured is a preserved shrimp fossil in the right upper corner. The soft-bodied features of the conodont are denoted in the schematic drawing (right). Photograph and schematic from Briggs et al. (1983).

## Biostratigraphic Application

Biostratigraphy is a branch of stratigraphy that uses fossils as a basis for subdividing, correlating, and establishing relative ages of sedimentary rock layers within and between depositional basins. To get a better idea of absolute age dates for biostratigraphic units, they must be related to the chronostratigraphic record. Gradstein et al. (2012) summarizes the techniques used for correlating biostratigraphic and chronostratigraphic data. Basically, a fossil assemblage is identified in a layer of rock and then correlated to an area where a rock layer with the same fossil assemblage exists and is bracketed, ideally, at its top and base by absolute age-date ranges.

In this discipline, index fossils are used to define and identify periods of geologic time. Ideal index fossils are those that are (1) easily distinguished from other taxa; (2) geographically widespread; (3) commonly found in most sedimentary rock types; and (4) restricted to a narrow interval of geologic time. The Mississippian Subsystem includes index fossils such as conodonts, brachiopods, crinoids, ammonoids, and foraminifera, which can be useful for age-dating. However, the Mississippian limestone has historically been difficult to study from a biostratigraphic perspective, particularly the Meramecian and Chesterian intervals (Godwin, 2017). In the Mid-Continent, conodonts have been the index fossil of choice for age-dating the Mississippian interval as they have shown the best regional correlation potential (e.g., Roundy, 1926; Stauffer, 1930; Gunnell, 1931; Stauffer and Plummer 1932; Thompson and Fellows, 1970; Mazzullo et al., 2011b; Boardman et al., 2013; Miller, 2015; Godwin, 2017, 2018; Hunt, 2017). Globally, Mississippian conodont biozones have temporal resolutions of about 3-4 m.y. (Gradstein et al., 2012). However, Godwin (2017) suggests that some Chesterian conodont biozones

within the U.S. Mid-Continent may represent a potential resolution of 1.8 m.y. It is not uncommon for a fossil group existing within a region to exhibit higher age-dating resolution when compared with global distributions of the same fossil group due to provincialism.

## Conodont Provincialism

Provincialism is simply the restriction of a population of fauna or flora to a geographic province. When exposed to selective environmental pressures over time, rapid evolution can occur among species in local populations due to adaptive responses. There are multiple lines of evidence to suggest provincialism occurred in Mississippian conodonts of the Mid-Continent (Gradstein et al., 2012). Previous studies have attributed various potential factors such as mass extinction events (Lauden, 1949), high-frequency sea-level fluctuations resulting from tectonics (Noble, 1993), basin restriction (Franseen, 2006), glaciation events (Buggisch et al., 2008), and a meteorite impact (Evans et al., 2011). However, a commonly accepted explanation regarding Mississippian conodont provincialism in the Mid-Continent remains inconclusive. The author of this study tends to agree with the opinions of Franseen (2006) and Hunt (2017) that basin restriction is the best encompassing explanation.

When referring back to the Blakey maps in Figures 6 and 7, the role tectonics played in creating restricted basin conditions can be inferred. These time slice figures give a sense of how the impending collision of Laurussia with Gondwana resulted in uplift and created regional barriers for ocean currents. The resulting seaway restriction in addition to high frequency sea-level fluctuations, may have contributed to minor mass

extinction events by influencing the supply of micronutrients of faunal groups, such as ammonoids and foraminifera, as suggested by Noble (1993), and the circulatory and salinity conditions (Russell, 2013; Hunt, 2017) contributing to localized disappearances of echinoderm and brachiopod families (Lauden, 1948; Ausich et al., 1994). Additionally, Evans et al. (2011) provide evidence suggesting a meteor impact occurred in present day southwestern Missouri around the time of the Osagean-Meramecian boundary, and that the event possibly played a role in the regional disappearances of echinoderm and brachiopod populations. Isolating basin conditions and events leading to minor mass extinction of certain faunal populations may help explain why biostratigraphic studies have been historically difficult for the Mississippian interval of the Mid-continent. However, these same conditions likely promoted provincialism among conodonts, resulting in rapid evolutionary divergence, allowing for regional high resolution conodont biostratigraphic analyses.

# CHAPTER IV

## DATA AND METHODS

The primary goal of this study was to age constrain Mississippian strata in the main STACK play and northwest extension using a combination of core-based conodont biostratigraphy and sequence correlations. Core descriptions were used to establish a sequence stratigraphic framework based on depositional facies and vertical stacking patterns. Detailed facies descriptions through thin section analyses were then used to refine and quantify those from core hand samples. Correlation of this framework to four principal conodont biozones provided relative age-dates of Mississippian intervals, which were subsequently related to electrofacies from wireline logs, then correlated to wireline logs in the STACK play proper in northwestern Kingfisher County, Oklahoma. This regional correlation was used to construct a cross section, illustrating the Mississippian stratigraphic architecture in the study area.

## Core Descriptions

The Pan American Barnes D-2 core consisting of 1,188 linear feet of slabbed core was made available for analysis at the Oklahoma Geological Survey Oklahoma Petroleum Information Center (OPIC). Core descriptions were performed using the Dunham (1962) classification of carbonate rocks according to depositional textures (Figure 12). From these descriptions, depositional facies were identified based on lithology, texture, grain size, sedimentary structures (lamination, bioturbation, and burrows), and fossil content. Following the methods of Flinton (2016) and Jaeckel (2016), similar facies were assigned numerical values and vertical stacking patterns were identified within depositionally significant packages. The stacking patterns were used to develop an idealized facies succession and establish a hierarchy of depositional sequences and cycles for the study area.

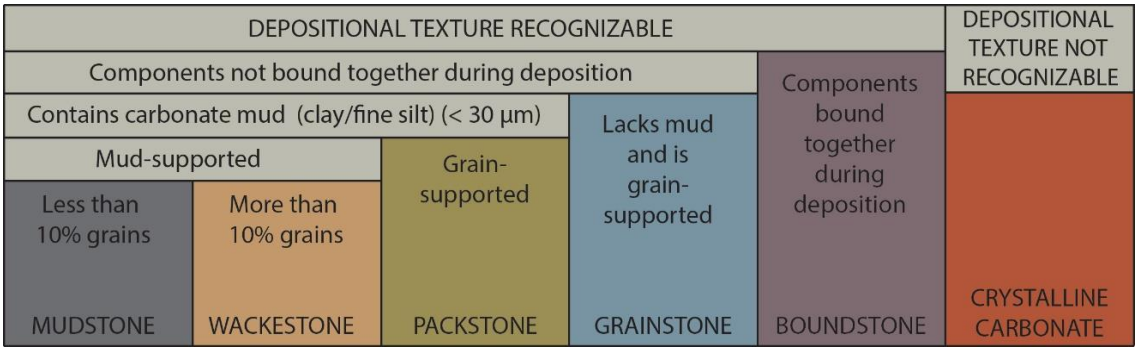


Figure 12. Diagram showing the Dunham (1962) classification of carbonate rocks according to depositional textures. Modified by LeBlanc (2014) after Scholle and Ulmer-Scholle (2003).

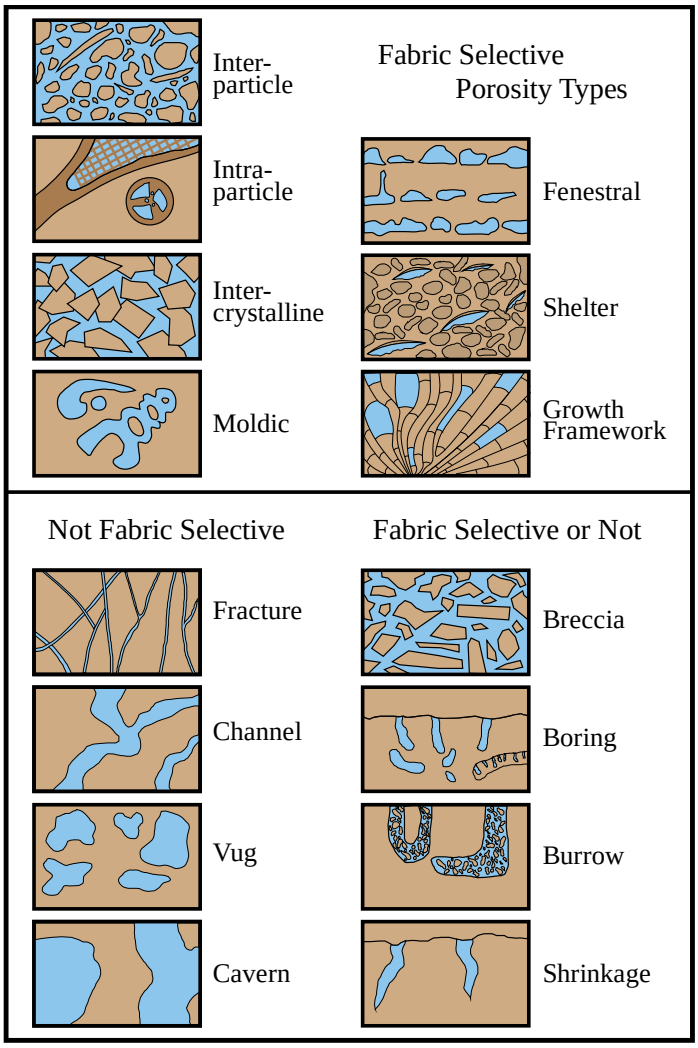


Figure 13. Diagram of the Choquette and Pray (1970) classification of fabric selective and non-fabric selective porosity types observed in carbonate rocks. Modified from Scholle and Ulmer-Scholle (2003).

## Petrographic Analysis

Petrographic analysis is necessary for identifying detailed variations that are not visible in hand samples, but may differentiate facies with distinct environmental indicators. Thin sections microscopy was performed to refine and quantify descriptions of hand samples.

In this study, 348 thin section photomicrographs, representing 45 thin sections from the Barnes D-2 core were supplied by OPIC. In addition to photomicrographs, the 45 core plugs were made available for thin section preparation as needed. Figure 14 shows the distribution of available photomicrographs and core plugs for this study. A cursory analysis was performed to identify photomicrographs for inclusion in this study based on their depths and correlation to generalized facies classification. Of the 45 plugs, 11 were selected for thin section preparation in intervals where photomicrographs were not available to represent all generalized facies types. As with core descriptions, thin section descriptions utilized the Dunham (1962) classification of carbonate rocks according to depositional textures (Figure 12) as well as the Choquette and Pray (1970) pore type classification scheme (Figure 13).

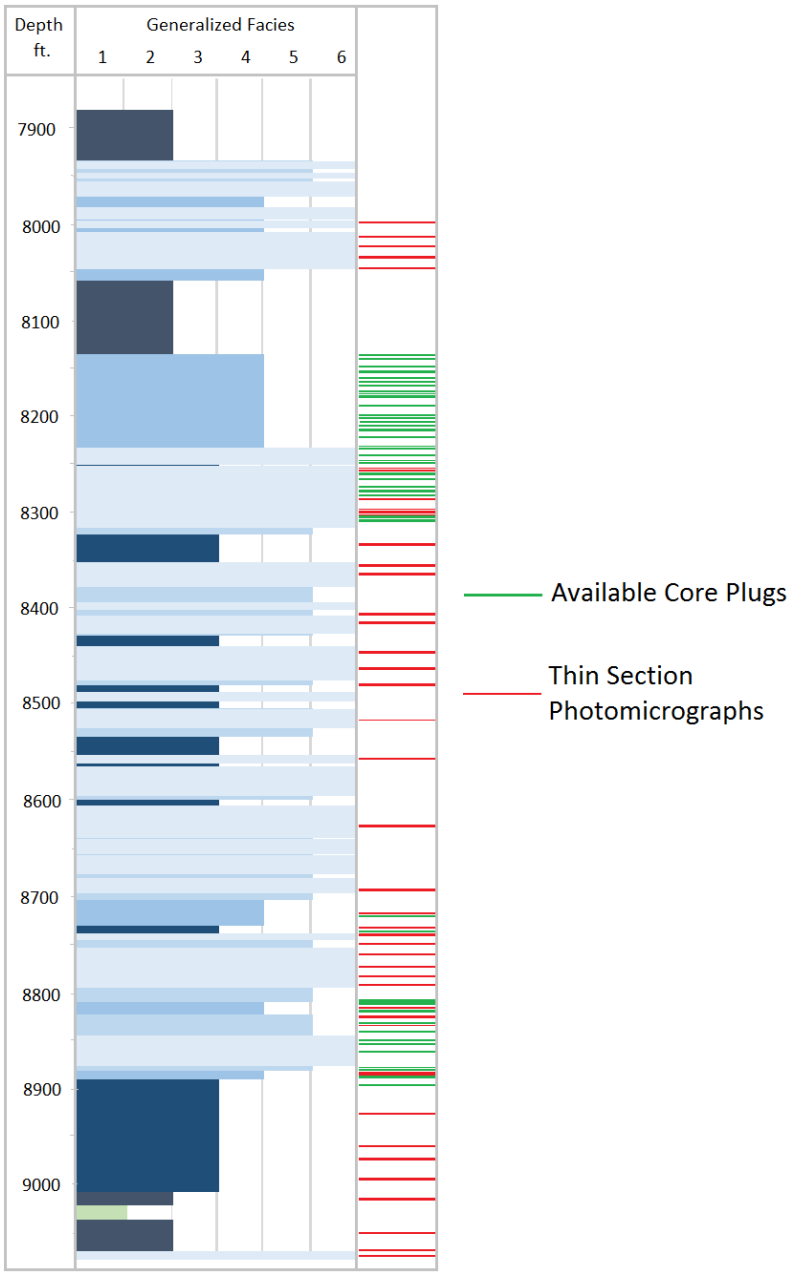


Figure 14. Generalized sampling summary for the Pan American Barnes Unit D-2 core. Horizontal axis shows generalized facies identified in core. Vertical axis shows true vertical depth measured in feet and the relative frequency of facies, which are described in Chapter IV. Also shown is the distribution of available thin section photomicrographs and core plugs across the Mississippian interval.

## Biostratigraphic Data

In refining outcrop stratigraphy of Meramecian and Chesterian strata in northeastern Oklahoma, Godwin (2018) identified four principal conodont biozones in rocks exposed along the western edge of the Mississippian outcrop belt. However, the lack of subsurface conodont data in the study area impairs our ability to apply these biozones to the subsurface. This not only inhibits our correlations and interpretations, it also hinders our overall understanding of the Mississippian stratigraphic architecture across the Anadarko basin.

In an effort to improve our understanding of subsurface biostratigraphy, Godwin (2018) evaluated conodont elements collected in the 1960s by AMOCO Research from the Pan American Barnes Unit D-2 core and archived at the University of Iowa. His evaluation revealed the presence of the same conodont biozones previously identified in the Mississippian outcrop belt, providing preliminary insight into the biostratigraphy of Mississippian intervals deposited within the Oklahoma basin and a mechanism for constraining the ages of Mississippian intervals in the STACK play of the Anadarko basin. Table 2 shows the conodont recovery from the Barnes D-2 core along with Godwin's (2018) principal biozones and equivalent formation names. Conodont taxa are listed across the top of the table while their occurrences are denoted by an "X." These data are organized by sample number in the left column with depth increasing as sample numbers become larger.

Figure 15 shows the lithostratigraphic nomenclature for the Upper Boone Group and the Mayes Group in the Tri-State Mining District and northeastern Oklahoma

(Godwin, 2017) compared with the nomenclature of Mazzullo et al. (2013). Dividing these stratigraphic columns are the four principal conodont biozones identified in the Mississippian outcrop belt by Godwin (2017). To maintain consistency with the stratigraphic nomenclature of this study, the biozones summarized below from Godwin (2017) will be referenced to the proposed nomenclature by Mazzullo et al. (2013). For example, Godwin (2017) states that Biozone 1 includes the Ritchey Formation and Tahlequah Limestone, so for consistency purposes, the Tahlequah Limestone will be omitted in the body of this text, although figures may still include the local formation names commonly used in the outcrop belt. However, it is important to note that a generalized lithostratigraphic framework may not precisely reflect the subsurface stratigraphy across the study area. For example, in the Mississippian outcrop belt, Biozones 2 and 3 are separated not only by their faunal differences, but also by the presence of a major sequence-bounding unconformity called the sub-Mayes unconformity (Godwin, 2017). In this case, subdividing the St. Louis Formation into upper and lower divisions lends to better temporal clarity (Figure 15).

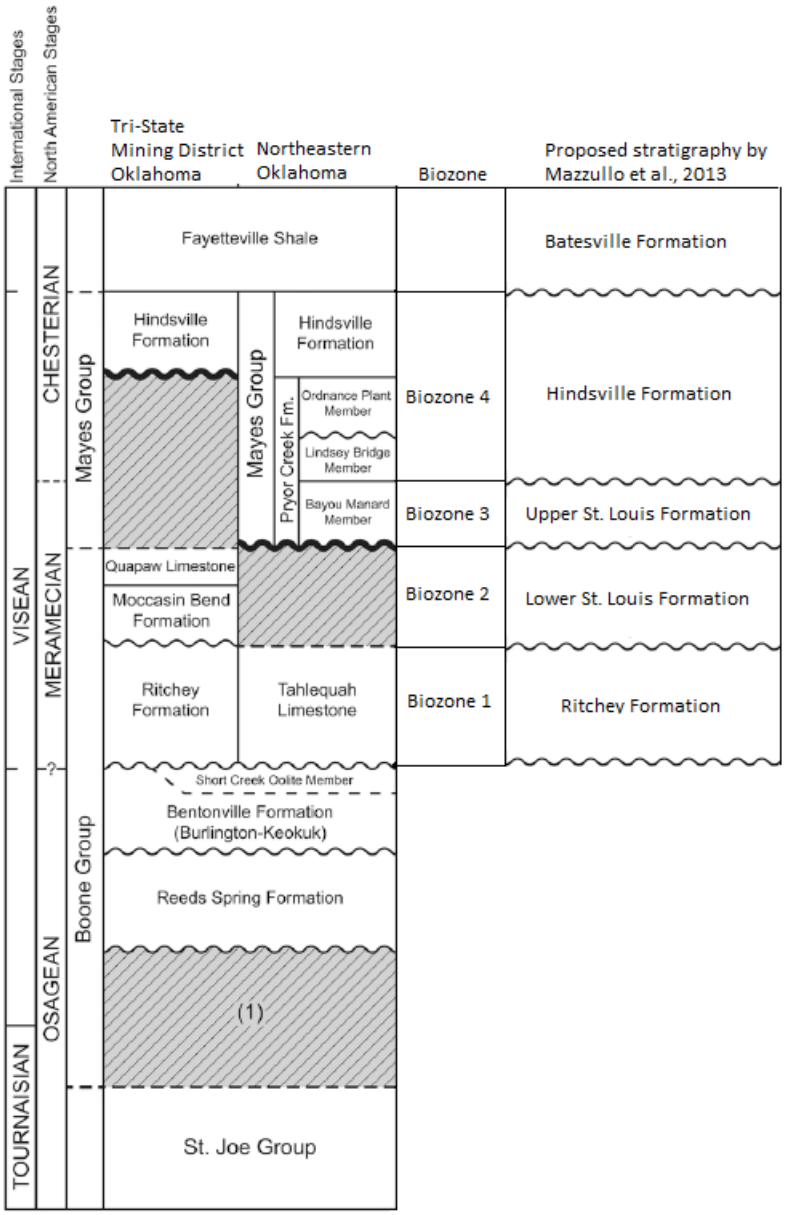


Figure 15. Comparison of lithostratigraphy of Tri-State Mining District and northeastern Oklahoma with that of a modified version of Mazzullo et al. (2013). Note that the St. Louis Formation has been subdivided in to upper St. Louis and lower St. Louis based on faunal differences and the presence of the sub-Mayes unconformity. Principal conodont biozones identified by Godwin (2017) are shown between the stratigraphic columns.

Table 2. Conodont recovery from the Barnes D-2 core in Major County, OK. Principal conodont biozones of Godwin (2018) with equivalent formation names are shown in the right hand column. The table is organized by sample number in the left column with depth increasing as sample numbers become greater. Modified from Godwin (2018).

| Sample No. | Depth (ft.) | Older Forms | *G. Texanus* | *G.pseudosemiglaber* | *L. homopunctatus* | *Taphrognathus* | *Transition form* | *Cavusgnathus* | *H.cristula* | *Hd. Spiculus* | *G. bilineatus* | Conodont Biozones |
|---|---|---|---|---|---|---|---|---|---|---|---|---|
| 45 | 7921.7-7922 | | | | | | | X | X | | | **Biozone 4** Chesterian |
| 100 | | | | | | | | X | | | | |
| 139 | | | | | | | | X | | | | |
| 170 | | | | | | | | X | | | | |
| 196 | | | | | | | | X | | | X | |
| 209 | | | X | | | | | X | | | | |
| 212 | | | X | | | | | X | | X | | |
| 275 | 8207.6-8208.2 | | | | | | | X | | | X | |
| 306 | 8236-8236.5 | | | | | | | X | | | | **Biozone 3** Upper St. Louis Fm. |
| 308 | | | | | | | | X | X | | | |
| 313 | | | | | | | | X | | | | |
| 316 | | | | | | | | X | | | | |
| 341 | | | | | | | | X | | | | |
| 351 | | | | | | | | X | | | | |
| 366 | | | | | | | | X | | | | |
| 370 | | | | | | | | X | | | | |
| 378 | | | | | | | | X | | | | |
| 395 | | | | | | | | X | | | | |
| 417 | | | | | | | | X | | | | |
| 437 | | | | | | | | X | | | | |
| 446 | 8379-8379.4 | | | | | | | X | | | | |
| 472 | 8395.1-8395.6 | | | | X | X | | X | | | | **Biozone 2** Lower St. Louis Fm. |
| 497 | | | | | | X | | X | | | | |
| 515 | | | | | | | X | | | | | |
| 575 | | | | | | | | X | | | | |
| 592 | | | | | | X | | X | | | | |
| 600 | | | X | | | | | | | | | |
| 610 | | | X | | | | | X | | | | |
| 623 | | | | | | | | X | | | | |
| 632 | | | | | | | | | X | | | |
| 637 | | | X | | | X | | X | | | | |
| 640 | | | X | | | X | | | | | | |
| 648 | | | X | | | X | | X | | | | |
| 659 | | | X | | X | X | | X | | | | |
| 672 | | | | | | X | | | | | | |
| 678 | | | | | | X | | X | | | | |
| 684 | | | X | | | X | | X | | | | |
| 687 | 8698.1-8698.7 | | | | | X | | X | | | | |
| 707 | 8741.3 | | X | X | | X | | | | | | **Biozone 1** Ritchey Fm. |
| 711 | | | X | X | X | X | | | | | | |
| 716 | | | | | | | | | | | | |
| 719 | | | X | | | X | | | | | | |
| 725 | | | X | | | X | | | | | | |
| 728 | | | X | | | X | | | | | | |
| 736 | | | X | X | | X | | | | | | |
| 742 | | | X | | | X | | | | | | |
| 746 | | | X | | | X | | | | | | |
| 751 | | | X | | | X | | | | | | |
| 755 | | | X | | | X | | | | | | |
| 760 | 8858.5-8859.5 | | | | | X | | | | | | |
| 832 | 9035? | X | | | | | | | | | | |

Summary of Principal Conodont Biozones Identified in Outcrop

Biozone 1 is interpreted as corresponding to the early to middle Meramecian Ritchey Formation. This zone is defined by the first and only occurrences of *Gnathodus* n. sp. 15 aff. *punctatus* (Boardman et al., 2013, pl. 15, fig 7; Godwin, 2017 pl. 1 fig C) and a potential newly identified species, *Gnathodus* sp. A (Godwin 2017, pl. 1 fig A). In addition to these defining species, Biozone 1 includes *G. pseudosemiglaber* (Godwin, 2017, pl. 1, fig M), *G. texanus*, and *G. linguiformis* and is marked by the first common occurrence of *Taphrognathus varians* (Godwin, 2017, pl. 1 fig D). The top of Biozone 1 is bound by the youngest observed occurrences of *Gnathodus* n. sp. 15 aff. *punctatus*, *G. pseudosemiglaber*, and *Gnathodus* sp. A. The stratigraphic range of Biozone 1 according to Godwin (2017) is identical to the upper *texanus*-*Gnathodus* n. sp. 15 aff *punctatus* zone of Boardman et al. (2013).

Biozone 2 is interpreted as representing the early to middle Meramecian lower St. Louis Formation. The base of Biozone 2 is characterized by the first observed occurrences of *Hindeodus cristula* and *Cavusgnathus* (Godwin, 2017, pl. 1). The top of this zone is characterized by the youngest occurrence of *Taphrognathus*. This zone can most easily be recognized by the co-occurrence of *Cavusgnathus* and *Taphrognathus* (Godwin, 2017; Lane and Brenckle, 2005). Biozones 1 and 2 together, were interpreted by Godwin (2017) to be roughly equivalent to the *Taphrognathus varians* – *Apatognathus* zone of Collinson et al. (1970) and the upper half of the *texanus* zone of Lane and Brenckle (2005).

Biozone 3 is interpreted to represent the late Meramecian Upper St. Louis Formation. In contrast to Biozone 2, Biozone 3 is recognized by the occurrence of *Cavusgnathus* without *Taphrognathus*, as well as the first occurrence of *Hindeodontoides spiculus* (Godwin, 2017, pl. 1, fig G). This zone was interpreted by Godwin (2017) to be roughly equivalent to the *Apatognathus scalensus-Cavusgnathus* Zone of Collinson et al. (1970) and the *scitulus-scalensus* Zone of Lane and Brenckle (2005).

The boundary between Biozones 3 and 4 marks a distinct faunal change and represents the Meramecian-Chesterian boundary (Maples and Waters, 1987; Godwin, 2017). Biozone 4 is characterized by the observed first occurrences of *Gnathodus bilineatus, G. girtyi girtyi*, and *Lochriea commutate* (Godwin, 2017, pl. 1 fig E, N, Q, and R), all of which are definitively Chesterian taxa (Godwin, 2017). Based on the first occurrences of these taxa, Godwin (2017) interprets Biozone 4 as generally equivalent to the early to middle Chesterian conodont zones of Collinson et al. (1970) and Lane and Brenckle (2005).

## Wireline Logs

Wireline logs measure and record physical attributes of rock within the borehole environment and are used to correlate wells based on their log signature as well as evaluate reservoir potential. Asquith and Krygowski (2004) provide a comprehensive overview of logging tools and their measurements. The information obtained from wireline logs, albeit practical and beneficial, cannot discern fundamental rock properties such as grain size, sedimentary structures, and texture. To effectively calibrate or “ground

truth" open hole logs to the core, wireline log signatures were correlated to their corresponding facies identified within the core.

Raster images of wireline logs acquired with the Barnes D-2 core, including gamma-ray, spontaneous potential, bulk density, formation density, and medium and deep resistivity open hole logs were provided by OPIC for use in this study. In addition to raster images, access to IHS digital log data, including gamma-ray and resistivity curves was provided by Midwest Land LLC. Using stratigraphic surfaces including radiogenic intervals on the gamma-ray curve, wireline logs were correlated by extrapolating away from the "ground truthed" log to identify the stratigraphic architecture across the study area. Thirty (30) digital wireline logs were selected and used to construct a cross section that illustrates the Mississippian stratigraphic architecture subparallel to paleodip. This cross section begins in Major County with the Pan American, Barnes D-2 in Section 23, T. 22N., R.16W., and terminates with the Pan American, Effie B. York well in Section 13, T.18N., R.09W., northwestern Kingfisher County.

# CHAPTER V

## FACIES ASSOCIATIONS

Six lithofacies were identified within the Mississippian interval of the Pan American Barnes D-2 core based on grain size and texture, sedimentary structures, color, and environmental indicators (Table 3). Analysis of thin sections and supplied photomicrographs were used to supplement and refine facies descriptions. The interpreted depositional environments represented with the core range from the deeper settings of the distal outer ramp to the more proximal higher energy settings of the upper mid-ramp to lower ramp crest (Figure 3). The depositional facies identified in the cored interval represent a generally shallowing upward system with an overall decline in sea-level across the Mississippian. The idealized facies succession begins with deposition of glauconitic shale during initial transgression. Shale and calcareous shale mark the deepest settings within the succession, followed by burrowed to bioturbated dolomitic wackestones-packstones with variations of chert-dominated to silt-dominated. As sea-level falls, deposition of relatively higher energy facies is indicated by more massive to traction-current laminated wackestones-packstones. Siliciclastic input into the system, marked by varying quantities of quartz silt, differentiates the silt dominated wackestone-packstone to calcareous siltstone from the massive to traction-current

laminated wackestone-packstone facies. As sea-level continues to fall, the presence of skeletal packstones-grainstones marks the highest energy facies within the idealized succession.

Table 3. Depositional facies identified from the Pan-American Barnes D-2 core. Sedimentological characteristics were derived from core descriptions. Primary grain types were derived from both core and thin section analyses. Bioturbation Index (BI) values were visually estimated from core data using the bioturbation index from Taylor and Goldring (1993).

| Facies | | Sedimentary Character | Primary Grain Constituents | BI (0-6) |
|---|---|---|---|---|
| 6 | Skeletal Packstone-Grainstone | Massive to planar cross-bedded lamination; skeletal debris; sparse bioturbation; low amplitude stylolites | Crinoids, Brachiopods, Sponge Spicules, Ooids, Bryozoa, Oncolites, Ostrocodes, Echinoderm fragements, Foraminifera | 0-1 |
| 5 | Wackestone-Packstone | Traction-current lamination in sections; hummocky cross-stratification; sparse to low bioturbation in sections; siliceous banding | Crinoids, Brachiopods, Sponge Spicules, Peloids; Bryozoa, trace Echinoderm & Foraminifera; Glauconite; Chert replaced / lined voids | 0-2 |
| 4 | Silty Wackestone-Packstone Calcareous Siltstone | Massive to suspension laminae in sections; periodic traction-current laminae; increased burrows in argillaceous sections | Sub-angluar to sub-rounded quartz silt, Crinoids, Brachiopods, Bryozoan, Peloids, rare oncolites; calcite cement | 0-2 |
| 3 | Bioturbated Dolomitic Wackestone-Packstone | Hoirizontally burrowed (mm scale) with suspension laminae to horizontally & vertically bioturbated (cm scale) with suspension to traction-current laminae | Dolomite, Carbonate replaced by chert in burrows, Quartz silt, Sponge spicules, Crinoids, Brachiopods | 3-5 |
| 2 | Shale-Calcareous Shale | Fissile shale grading to massive calcarous shale; Horizontal burrows present in areas and not apparent in others; Mineralized fractures | Dolomite, Pyrite, Illite, Quartz, Micrite | 0-1 |
| 1 | Glauconitic Shale | Massive bedding to suspension laminae; burrowed; silica filled vugs | Glauconite grains, thin-shelled brachiopod fragments | 0-2 |

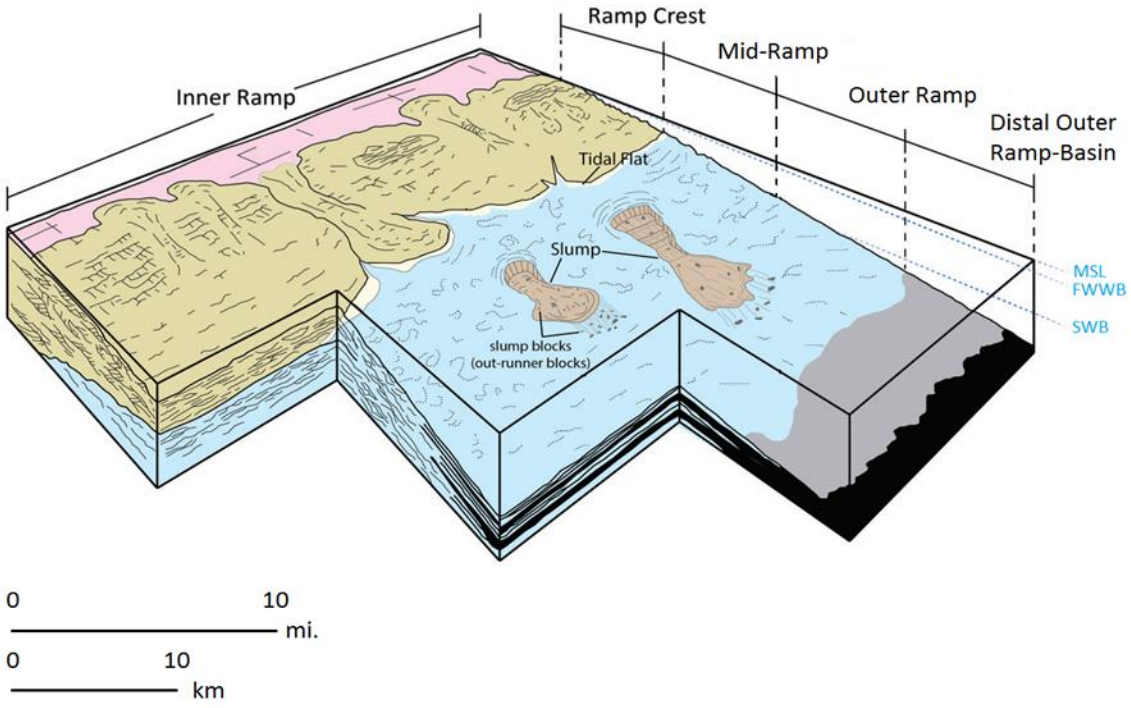


Figure 16. Schematic diagram of ramp environment illustrating the distribution of depositional facies. Modified from Childress (2015) after Handford (1986).

Facies 1: Glauconitic Shale

The glauconitic shale facies (Figure 17) is a burrowed, dark olive green to greenish-gray calcareous shale. The base of the green shale is in sharp contact with the underlying black fissile Woodford Shale. The upper contact is gradational with the overlying gray calcareous shale of facies 2. Thin sections nor photomicrographs were available for analyses for this study. However, descriptions by Flinton (2016) of core and thin sections from the Droke Unit # 1 within the study area in northwestern Kingfisher County, Oklahoma, reveal this facies is composed of sub-rounded and poorly sorted glauconitic grains in a calcareous matrix. The sandstone unit (not apparent in the Barnes D-2 core) of this facies displays partial moldic and vuggy porosity after glauconite grains

with very rare shelter porosity beneath thin-shelled brachiopods (Flinton, 2016). Locally, the core exhibits rare silica filled vuggy porosity (cm scale).

Glauconite is an iron and potassium rich phyllosilicate mineral, authigenically formed in submarine reducing environments with very low to negligible sedimentation rates (Middleton et al., 2003). This facies is present in the lowermost portion of the core, which is consistent with regional studies (LeBlanc, 2014; Flinton, 2016). Based on the presence of glauconite and observations above, facies 1 is interpreted to represent deposition during initial transgression in a restricted, low energy environment.

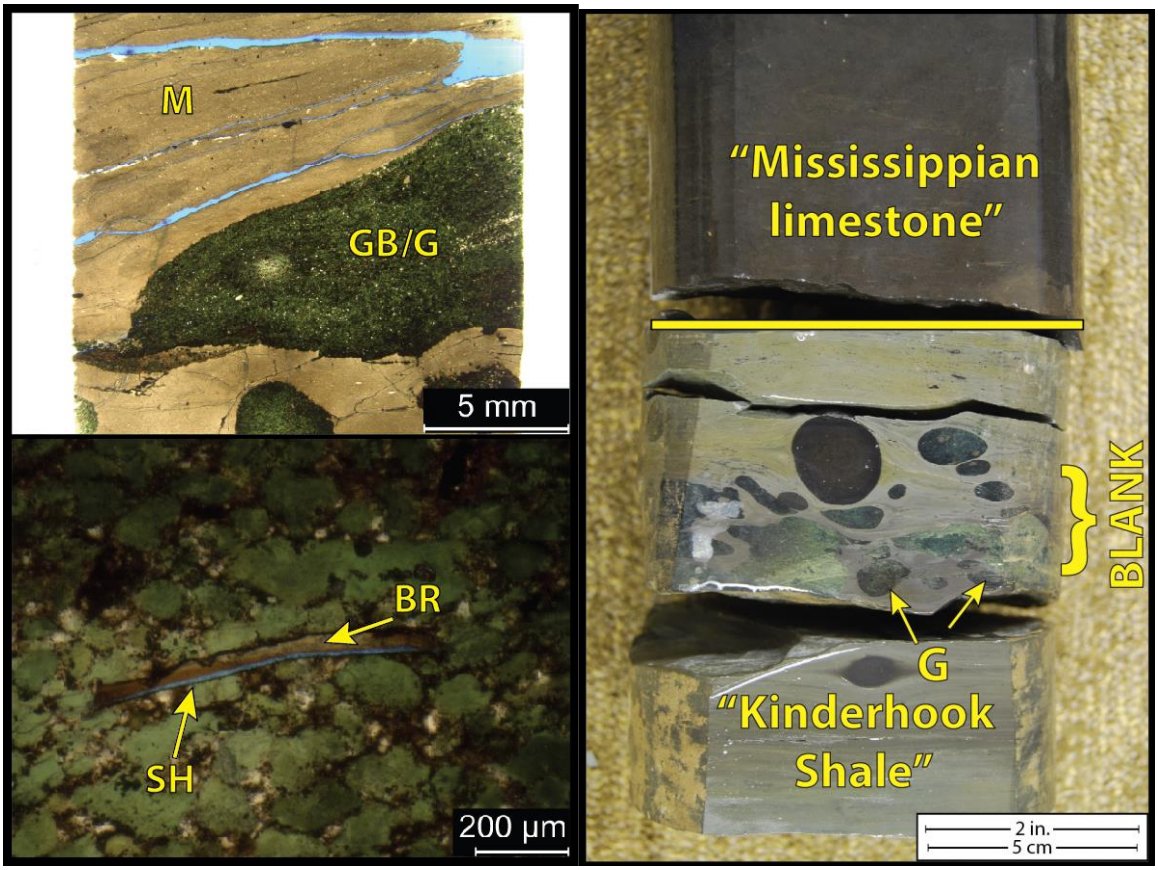


Figure 17. Facies 1: Glauconitic Shale. Thin section photomicrographs (left; plane polarized light (PPL)) and corresponding core photograph (right) from the Droke Unit #1 in northwestern Kingfisher County, OK. Core photograph shows glauconitic grains (GB/G) in a calcareous shale matrix (M). Shelter porosity (SH) beneath a thin-shelled

brachiopod (BR) in thin section (bottom left). Figure representative of Facies 1 within the study area. From Flinton (2016).

Facies 2: Shale – Calcareous Shale

The shale-calcareous shale facies (Figure 18) consists of gray to dark gray calcareous and occasionally silty shale and pyritic black shale. Sedimentary structures include very thin horizontal suspension laminae. Shale in the lower portion of the core display periodic and rare millimeter scale burrowing, likely *Cruziana*- or *Zoophycos*-type, commonly replaced by chert. Few brachiopod and undifferentiated skeletal fragments were also observed in the lower portion (9,000-9,019 ft.). A predominantly illite matrix was observed in thin section at a depth of 9,017.25 ft. Shale in the upper portions of the core (8,137.5-8,056 ft.) tend to grade from dark gray and calcareous with no apparent burrows, to lighter gray with increasing carbonate content and burrowing. Periodic fissility is common. Both upper and lower contacts of facies 2 tend to be gradational.

Facies 2 is interpreted to represent deposition within the distal outer ramp to basin environment as sea-level continued to rise. The presence of fine suspension laminae indicates a low energy environment, while the presence of pyrite combined with the limited diversity and occurrence of organisms (mm scale burrows, thin-shelled brachiopods, and few undifferentiated skeletal fragments) suggests a fluctuating environment between dysoxic and periodically oxygen enriched (Ekdale et al., 1984).

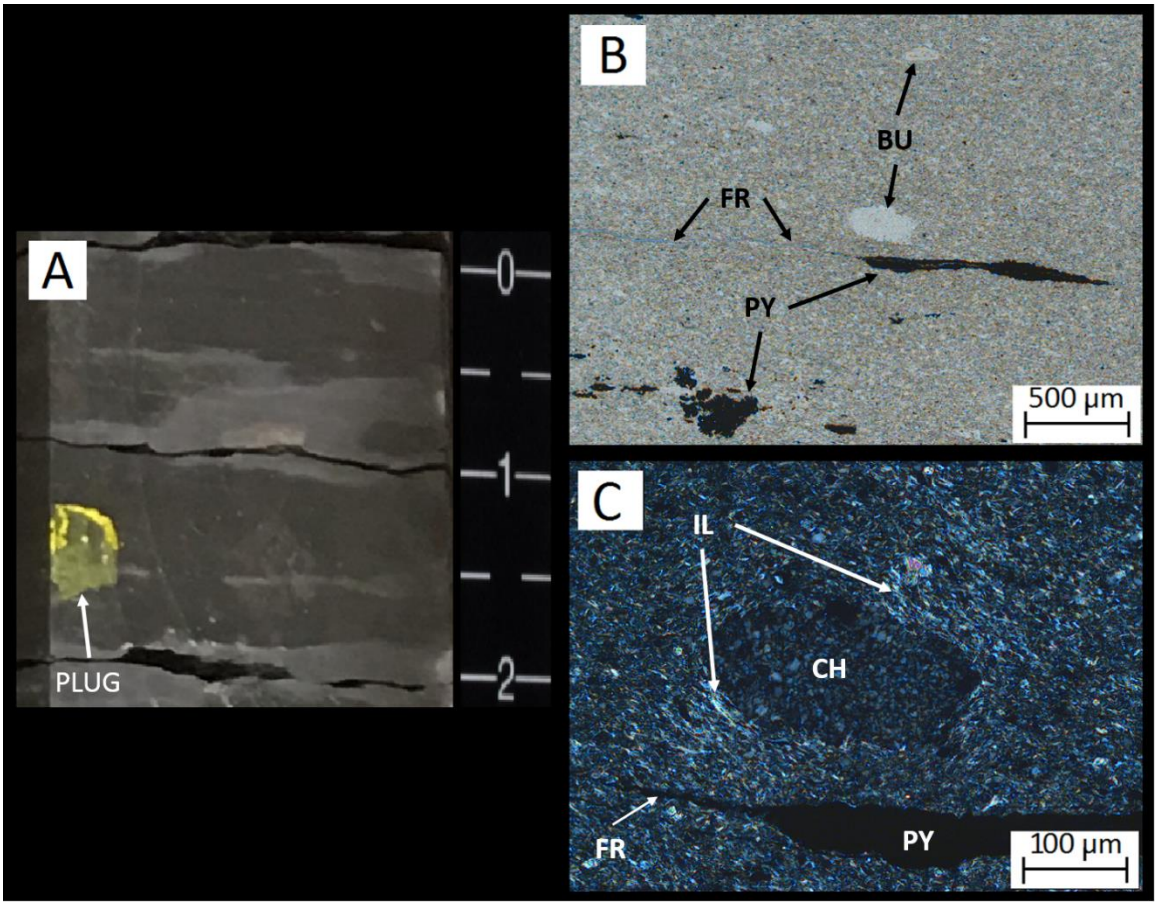


Figure 18. Facies 2: Shale-Calcareous Shale. A) Core photograph of facies 2 from the Barnes Unit D-2 core at a depth of 9,017.25 ft. Scale for core photo is in tenths of feet; yellow paint on core sample marks thin section (B & C) location. Thin section photomicrographs of facies 2 in PPL (B) and cross polarized light (XPL) (C) from depth of 9017.25 ft. Thin section displays an illite (IL) rich mud matrix with chert (CH) filling burrows (BU) and pyrite (PY) filling a fracture (FR).

Facies 3: Bioturbated Wackestone-Packstone

The bioturbated mudstone to wackestone-packstone facies (Figures 19 & 20) is a dolomitic carbonate facies containing a considerable microcrystalline quartz. Also present within this facies are thin-shelled brachiopods, sponge spicules, undifferentiated skeletal fragments, quartz silt, ostracods, and pyrite in a micrite matrix. This facies

displays moderate to intense bioturbation resulting from individual centimeter scale vertical and horizontal burrows, likely *Cruziana*- or *Skolithos*- type (BI = 3-5). Burrows appear to have provided pathways for siliceous fluids to permeate this facies, which promoted secondary replacement of carbonate material with microcrystalline quartz, referred to as chert (Figure 19). In the lower portion of the core, most notably from 8,980 – 8,885 ft., the microcrystalline quartz is predominantly spicular chert, as sponge spicules are commonly observed to be concentrated within these chert replaced voids. Franseen (2006) suggests upwelling from basinal waters during the early Mississippian may have been the primary mechanism for delivering nutrients and dissolved silica, thus promoting the proliferation of siliceous sponges across the region.

Facies 3 is interpreted as outer ramp to distal outer ramp sediments deposited in a low to moderate energy environment at or below storm wave base (SWB) (Figure 16). Although moderately to intensely bioturbated, bedding boundaries still appear distinct in some areas displaying traction-current laminae to suspension-laminated mud wisps indicating periodic storm influence. A moderate increase in faunal diversity and a high degree of bioturbation suggests well-circulated, normal marine conditions.

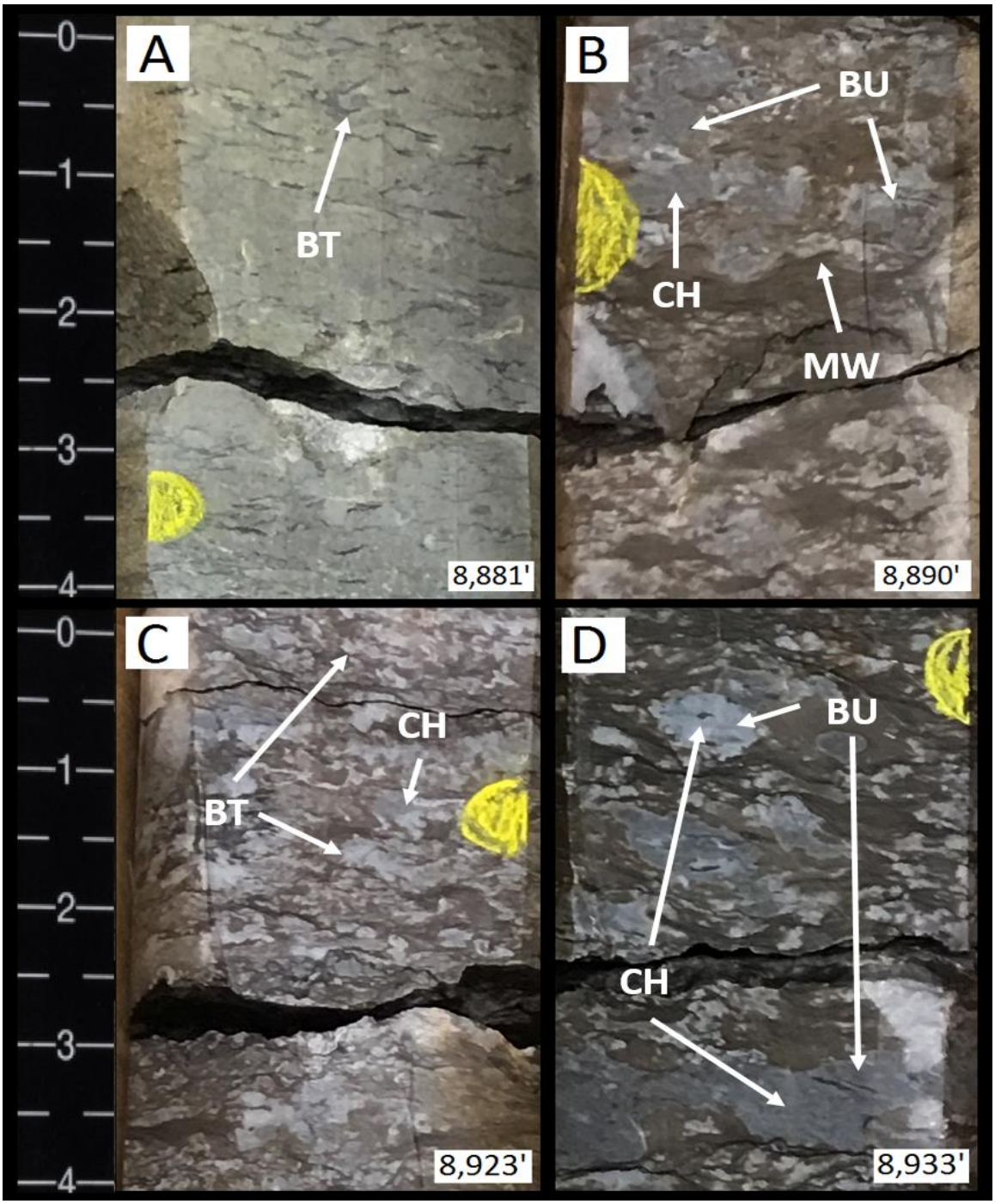


Figure 19. Facies 3: Bioturbated Wackestone-Packstone. A, B, C, & D) core photographs depicting the varying degree of bioturbation due to burrowing within Facies 3. Relatively larger individual burrows (BU) are recognized in C & D. The figure also shows microcrystalline quartz, or chert (CH; blue-gray material) replacing carbonate material in burrows. Scale for core photos is in tenths of feet; yellow paint on core samples mark thin section locations (Figure 20 A, B, & C).

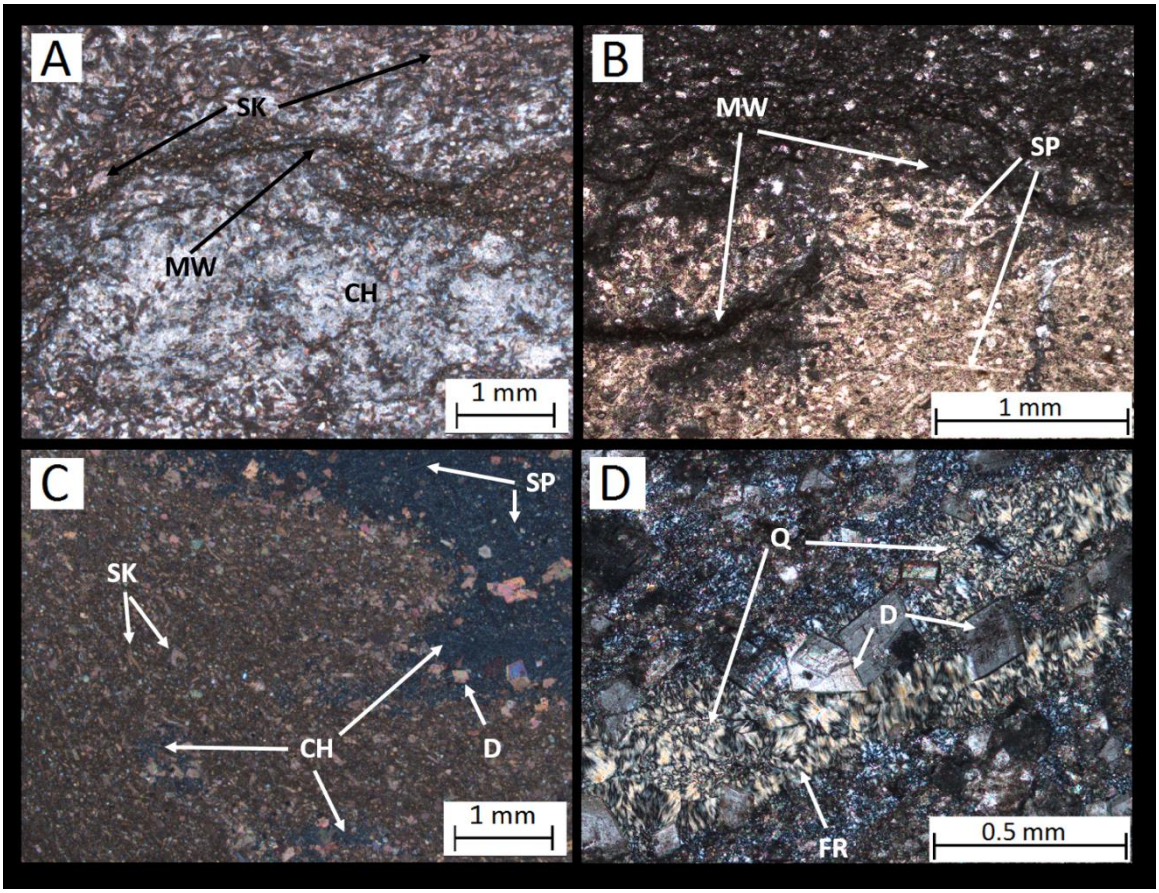


Figure 20. Facies 3: Bioturbated Wackestone-Packstone. Thin section photomicrographs at depths of: A) 8,881 ft shown in PPL at 2.5X magnification. Skeletal grains (SK), mud wisps (MW), chert (CH) displayed; B) 8,890 ft shown in PPL at 2X magnification. Note sponge spicules (SP) in chert (yellowish- tan in color); C) 8,923 ft shown in XPL at 2.5X magnification. Dolomite (D), skeletal grains and chert (CH); and D) 8,805 ft shown in XPL at 2X magnification, displaying chalcedony (Q) filled fracture (FR) and dolomite (D).

Facies 4: Silty Wackestone-Packstone to Calcareous Siltstone

The silty wackestone-packstone (Figure 21) to calcareous siltstone is a transitional facies between facies 3 and 5, characterized by varying, but significant input of detrital quartz silt. The varying degree of silt input essentially bifurcates Facies 4 into two distinct presentations. In the upper portion of the core (above 8,240 ft) facies 4 presents

as calcareous siltstone composed of predominantly sub-angular to sub-rounded quartz silt with peloidal grains, crinoids, brachiopods, bryozoa, and undifferentiated carbonate skeletal grains in calcite cement (Figure 21). It is moderately to well sorted and dominated by massive bedding to suspension lamination with periodic traction-current planar lamination and hummocky cross-stratification. In the lower portion of the core (below approximately 8,700 ft), facies 4 presents as a continuation of facies 3, but with increased silt content. Chert is still present in facies 4 and seemingly preferential to bioturbated and burrowed intervals. An inverse relationship is observed to exist between the presence of silt and chert. It appears that as the abundance of silt increases, the amount of chert decreases.

Facies 4 is interpreted as outer ramp to distal outer ramp sediments deposited in a low to moderate energy environment at or below SWB (Figure 16). An increase in faunal abundance, diversity (brachiopod, bryozoa, and crinoids), and size (~0.5-1.5 mm) of skeletal material suggests normal marine conditions and a relatively higher energy depositional environment than Facies 3.

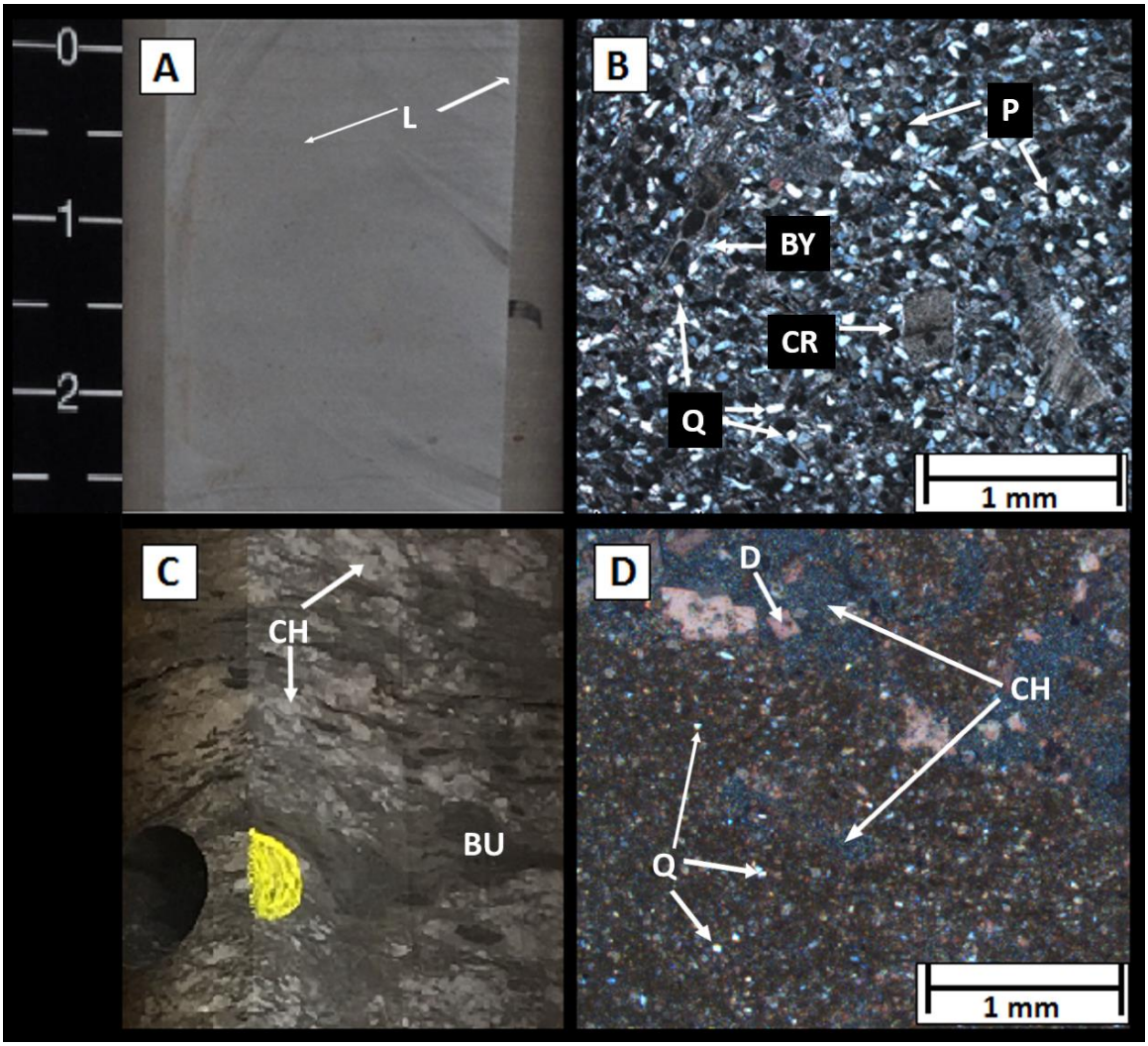


Figure 21. Facies 4: Calcareous Siltstone to Silty Wackestone-Packstone. Core photographs (A&C) with corresponding thin-section photomicrographs (B&D, respectively). A and B are representative of the calcareous siltstone facies from 8206 ft, C and D are representative of the silty wackestone-packstone facies from 8715 ft. A) Suspension lamination (L) with periodic traction-current laminae (not depicted) is common within the silt-dominated areas of Facies 4; B) Bryozoa (BY), crinoids (CR), and peloids (P) within calcite cemented siltstone. Quartz grains (Q) vary between silt to sand size in Facies 4; C and D) Silty wackestone-packstone facies at 8715 ft. Continuation of Facies 3, but with relatively higher abundance of quartz silt. Scale for core photos is in tenths of feet; yellow paint on core sample (C) marks thin section location (D).

Facies 5: Traction-Current Wackestone-Packstone

The traction-current wackestone-packstone facies (Figure 22) is composed of sponge spicules, brachiopods, crinoids, peloids, bryozoa, trace echinoderms and foraminifera, and undifferentiated skeletal debris. Siliceous banding from concentrations of chert is commonly observed in core (Figure 22 A), while thin-sections display chert filling voids and lining porosity (Figure 22 C). Traction-current lamination is common in facies 5, displaying planar cross-lamination, hummocky cross-stratification, and argillaceous areas with fine planar lamination.

Facies 5 is interpreted as mid-ramp sediments deposited in moderate energy environment between FWWB and SWB (Figure 16). The faunal diversity observed in facies five suggests a well-oxygenated environment with normal marine conditions during deposition. Traction-current lamination and the disaggregated nature of skeletal grains suggest periodic reworking by storms.

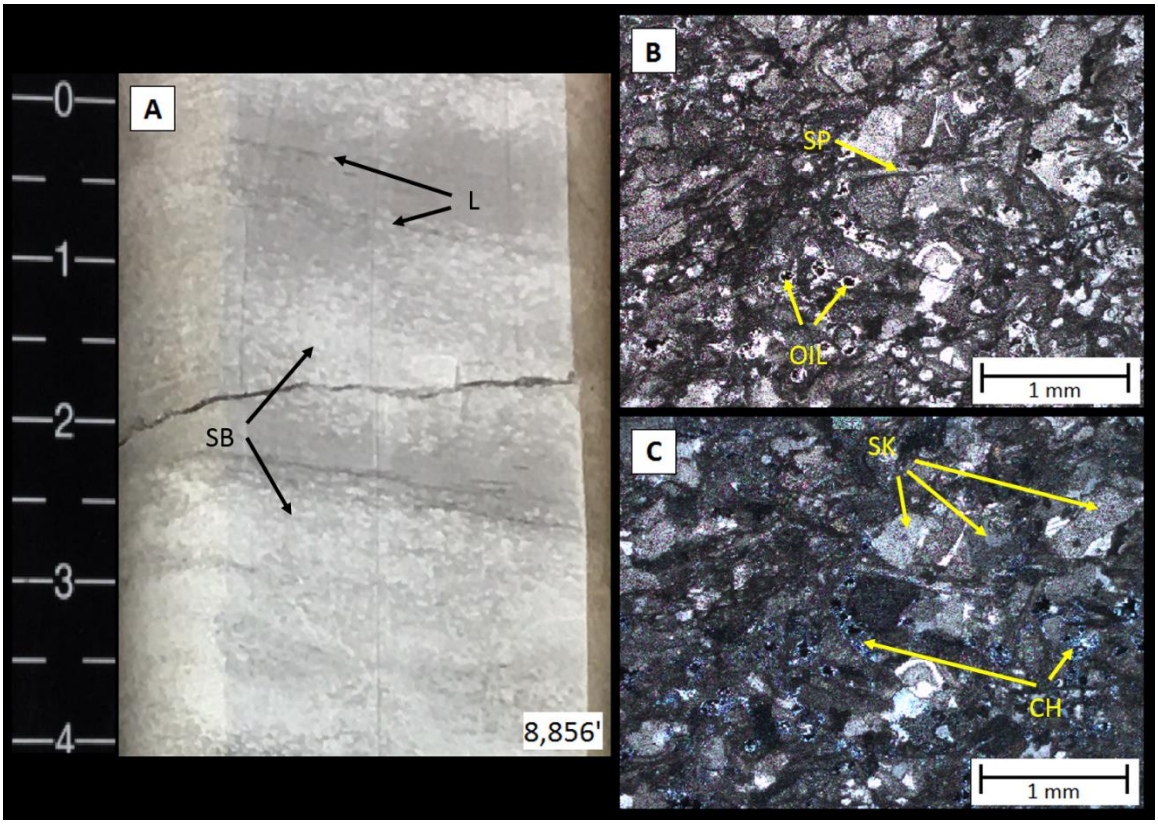


Figure 22. Facies 5: Traction-Current Wackestone-Packstone. Core photograph (A) from the Barnes D-2 core at a depth of 8,856 ft., Siliceous banding (SB) and traction current laminae (L); representative of the facies displayed in thin-section photomicrographs (B and C) from a depth of 8,858 ft. Figures (B) and (C) are displayed under 2X magnification with (B) shown in plane-polarized light and (C) shown in cross-polars. Sponge spicules (SP) and skeletal fragments (SK) are noted, while dead oil (OIL) is observed in moldic and vugular porosity lined with chert (CH).

Facies 6: Skeletal Packstone-Grainstone

The skeletal packstone-grainstone facies (Figure 23) is a grain dominated facies characterized by skeletal material consisting of crinoids, brachiopods, echinoderms, bryozoa, ostrocodes, sponge spicules, foraminifera, and undifferentiated skeletal grains. Calcite cementation of larger grains is variably observed as shown in Figure 23D. The upper right corner of Figure 23D displays syntaxial calcite overgrowth on an original

crinoid grain. Sub-rounded to sub-angular quartz silt is variably present (Figure 23B), but to a lesser degree than observed in facies 4.

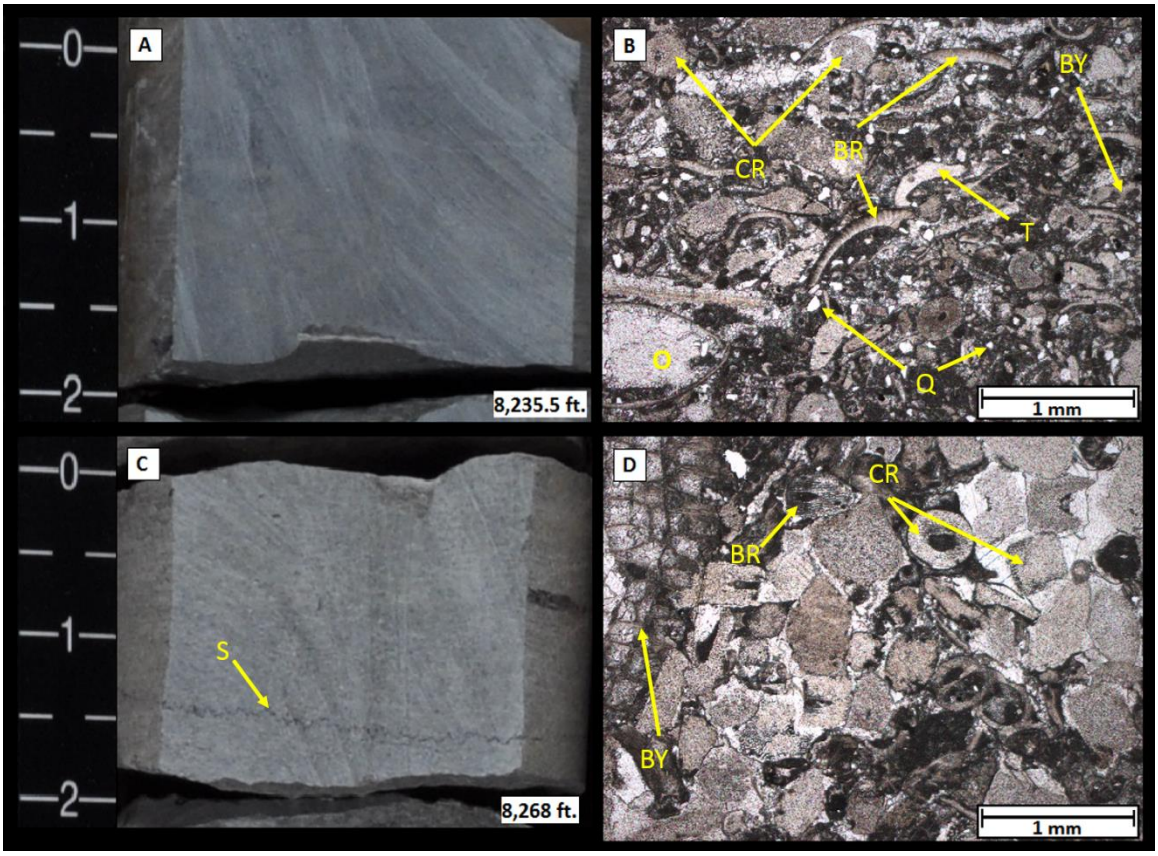


Figure 23. Facies 6: Skeletal Packstone-Grainstone. Core photographs (A and C) with corresponding thin-section photomicrographs (B and D, respectively). Figures (B) and (D) are both displayed in 2X magnification under PPL and show grains commonly observed in facies 6, such as disaggregated crinoids (CR), bryozoa (BY), brachiopods (BR), ostrocodes (O), trilobite fragments (T), and quartz silt (Q).

Facies 6 is interpreted as mid-ramp to distal-ramp-crest sediments deposited near FWWB. The presence of cross-bedding and planar lamination suggest a relatively high energy environment. The high degree of faunal diversity and abundance of skeletal grains indicates a well-oxygenated environment with normal marine conditions at time of deposition. The sedimentary character of traction-current deposition with the grain diversity and abundance suggests these sediments may represent the down ramp margin of an active skeletal shoal complex.

# CHAPTER VI

# RESULTS

## Sequence Stratigraphic Framework

### Idealized Facies Succession

A sequence stratigraphic framework was developed for the Mississippian section of the Barnes D-2 core based on vertical stacking patterns of depositional facies described in the previous chapter. Vertical stacking patterns result from lateral shifts in depositional facies, landward or basinward, due to relative and eustatic sea-level changes. The idealized vertical facies succession (Figure 24) represents one complete rise and fall of sea-level, with the blue triangle representing the transgressive phase and the red triangle representing the regressive phase. In the study area, the idealized facies succession exhibits a relatively rapid transgressive phase followed by a gradual shallowing-upward regressive phase, resulting in an overall shallowing-upward sequence. This idealized stacking pattern was used to identify a hierarchy of depositional sequences and cycles.

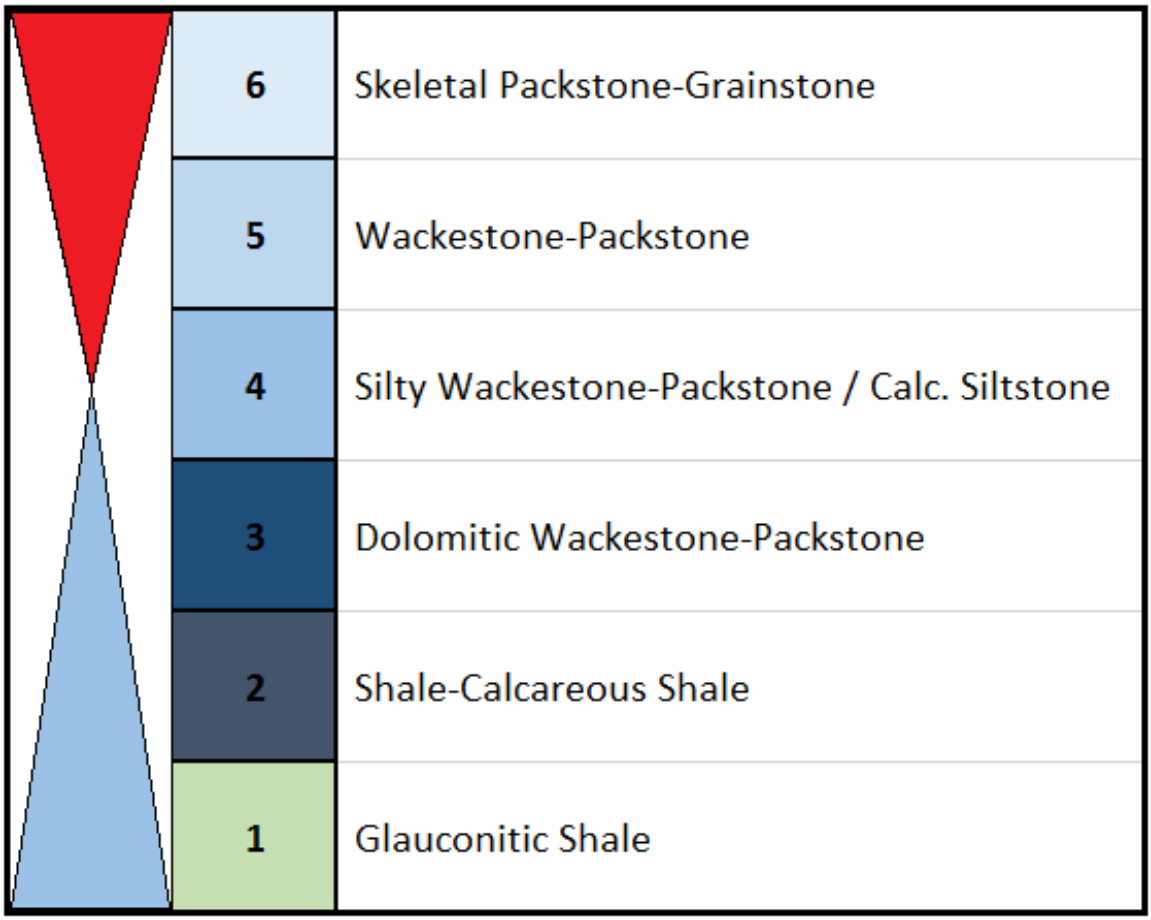


Figure 24. Idealized vertical facies succession identified in the Pan-American Barnes D-2 core in Major County, Oklahoma. This facies stacking pattern is representative of depositional facies encountered during one complete rise and fall in sea-level. The transgressive phase is represented by the blue triangle, while the regressive phase is represented by the red triangle.

Sequence Stratigraphic Hierarchy

The Mississippian section in the study area is interpreted to represent a 2nd order, overall shallowing-upward supersequence. The Barnes D-2 core is an incomplete representation of this 2nd order supersequence as the cored interval begins at the top of the Woodford Shale and terminates in the "Chester Shale" below the Mississippian-Pennsylvanian boundary.

The cored interval demonstrates three levels of cyclicity within this 2nd order supersequence. These 3rd-, 4th-, and 5th- order sequences and cycles represent their position in the stratigraphic hierarchy, illustrating the relative increase in frequency. Five 3rd order depositional sequences (S1-S5) are recognized within the Barnes core from the top of the Woodford Shale to the lower Chesterian (Figure 25). These observed 3rd order sequences each display shallowing-upward character and are regionally correlative. Referring back to Table 1, 3rd order sequences have an approximated duration of 1 to 10 m.y. Conodont biostratigraphic data available for this study provided relative time-constrained divisions or "biozones" which aided in defining these 3rd order sequences, revealing an average duration of 2.7 m.y. (Godwin, 2017).

In S3, multiple 4th and 5th order high-frequency sequences (HFS) and cycles (HFC) are observed, indicating a period of relatively rapid sea-level fluctuation, likely resulting from Milankovitch-band glacioeustacy driven by eccentricity (4th order) and obliquity and precession (5th order) (Read, 1985). Although HFSs (4th order) and HFCs (5th order) are below the resolution provided by current conodont biostratigraphic data, conodont biozones can provide temporally-constrained boundaries for interpretations relating to higher frequency cyclicity.

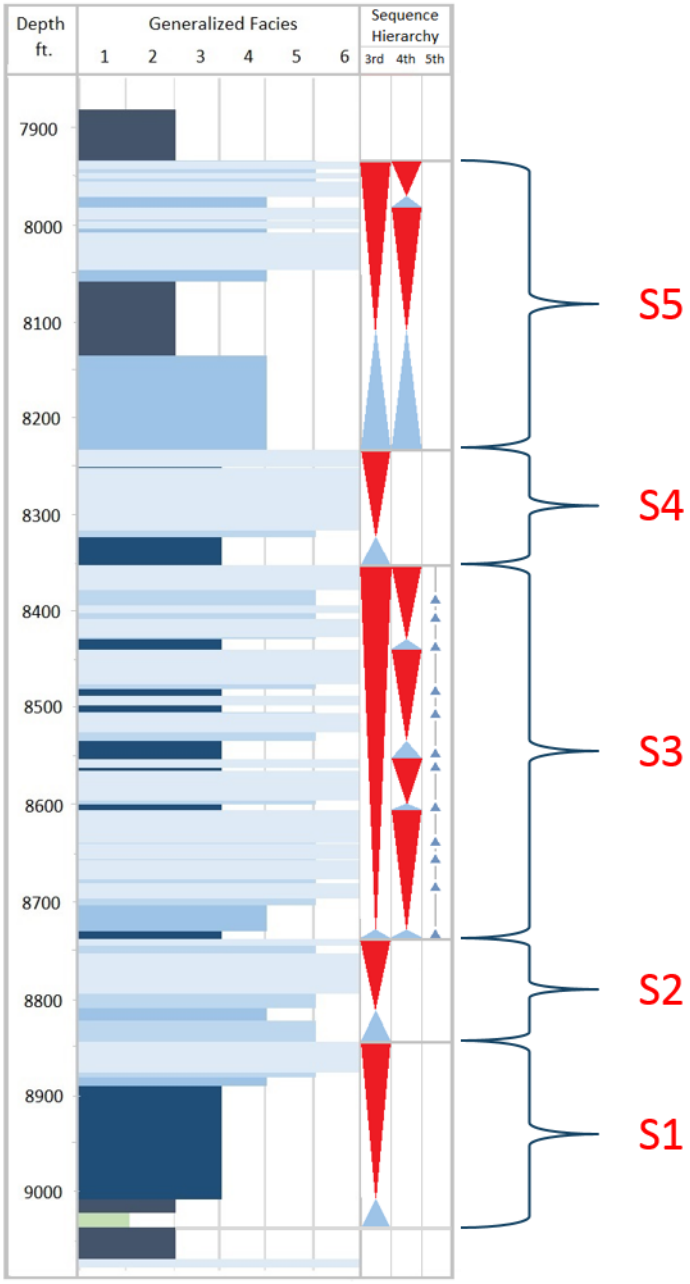


Figure 25. The sequence stratigraphic hierarchy of the Mississippian interval in the Barnes D-2 core displays four levels of sea-level cyclicity (2nd through 5th order). The entire cored interval represents a partial 2nd order shallowing-upward supersequence, as the cored interval for this study did not extend to the Mississippian/Pennsylvanian unconformity. Five 3rd order depositional sequences (S1 – S5) with shallowing-upward signatures were observed with 4th order HFSs and 5th order HFCs variably recognized (S3 and S5).

## Conodont Biostratigraphy of the Barnes D2 Core

### Notable Conodont Taxa

Godwin's (2018) biostratigraphic evaluation of the Barnes D-2 core revealed notable conodont taxa previously identified in the Mississippian outcrop belt. Based on Godwin's (2017) principal conodont biozones, the recovery of distinct conodont taxa (Table 2) from the Barnes D2 core, provides a mechanism for constraining the relative ages of Mississippian intervals in the STACK play of the Anadarko basin.

Useful age diagnostic conodont species used to constrain age boundaries in the Barnes D-2 core include the following: (1) *Taphrognathus varians* in the middle part of the second 3rd order sequence (S2), corresponding to Biozone 1 of the early Meramecian; (2) *Gnathodus pseudosemiglaber* in the upper portion of the second 3rd order sequence (S2), corresponding to Biozone 1; (3) *Taphrognathus varians*, (4) *Cavusgnathus unicornis* and (5) *Lochriea homopunctatus* in the upper part of the third 3rd order sequence (S3), corresponding to Biozone 2 of the middle to upper Meramecian; (6) *Cavusgnathus unicornis* in the mid to upper portion of the fourth 3rd order sequence (S4), corresponding to Biozone 3 of the late Meramecian; (7) *Hindeodus cristula* and (8) *Gnathodus bilineatus* in the lowermost portion of the fifth 3rd order sequence (S5), corresponding to Biozone 4 of the early Chesterian; and (9) *Cavusgnathus regularis* in the middle of the fifth 3rd order sequence (S5), corresponding to the Chesterian Biozone 4. See appendix A for conodont plates according to biozone, displaying notable species from both the Barnes D-2 core and those recovered from the Mississippian outcrop belt.

Identification of notable conodont taxa listed above, provides a "no older than" or "no younger than" basis and allows estimates of ages of Mississippian intervals within

the study area. For example, Godwin (2017) explains that the recovery of *Taphrognathus* indicates the cored section is no older than Osagean. Likewise, when *Cavusgnathus* is recovered, we know the sample is no older than mid to upper Meramecian. Godwin's (2017) principal biozones are evident in the Barnes D-2 core and can be delineated as follows: (1) Biozone 1, which is based on an abundance of *Taphrognathus* relative to other taxa; (2) Biozone 2 that is based on the co-occurrence of *Taphrognathus* and *Cavusgnathus*; (3) Biozone 3 which is indicated when there is recovery of *Cavusgnathus* without *Taphrognathus;* and (4) Biozone 4 that is based on the recovery of definitive Chesterian species, such as *Gnathodus bilineatus*. Figures 26-29 show these notable taxa recovered from the Barnes D-2 core with their corresponding species recovered from outcrop, if available. Figure 30 presents a summary of biostratigraphic and sequence stratigraphic results, showing the notable conodont taxa recovered from the Barnes D-2 core. These data reveal that Mississippian intervals below the "Chester Shale" range primarily from early Meramecian (Biozone 1) to middle Chesterian (Biozone 4). The contact between the Meramecian and Chesterian ages was identified honoring biostratigraphic constraints. The Meramecian-Osagean boundary however, could not be resolved due to limited conodont recovery. Osagean rocks may still be present in the approximately 200 ft of Mississippian carbonate section below the first identified biozone.

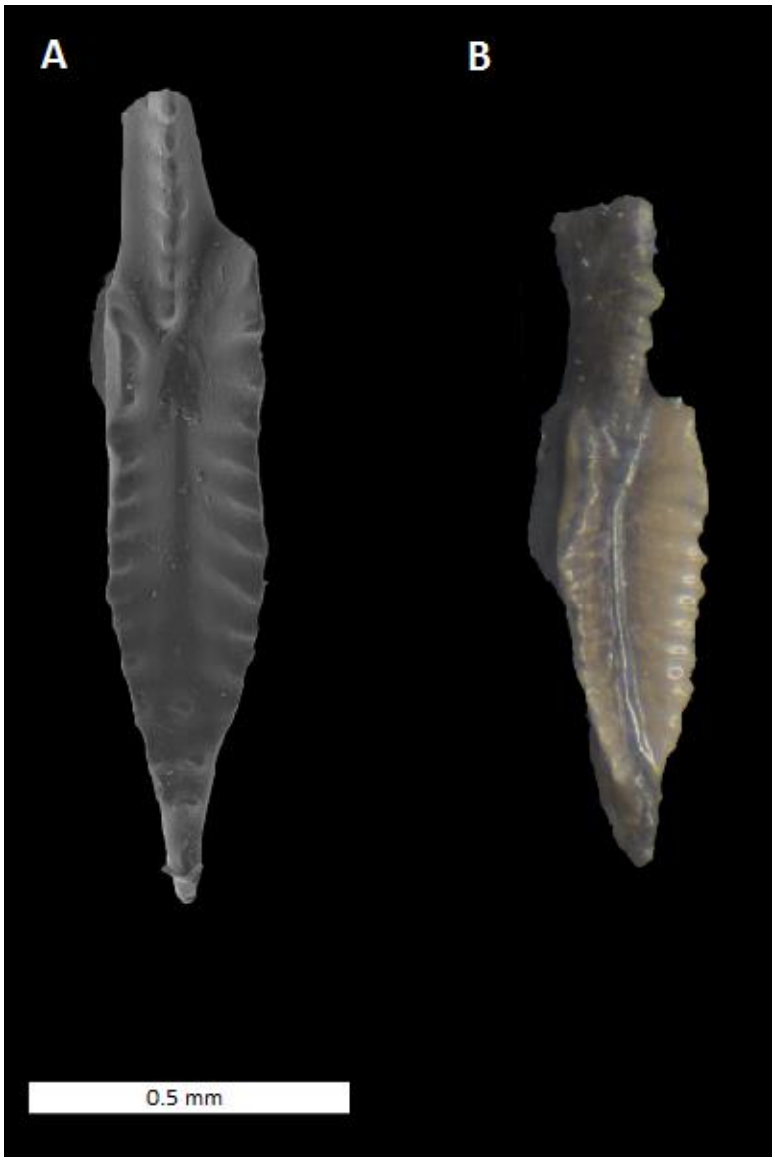


Figure 26. SEM image (A) and macrophotograph (B) of *Taphrognathus* recovered from Ritchey Formation, Boone Group, Ottawa County, OK and the Barnes Unit D-2 at a depth of 8786.4-8786.9 ft (specimen not to scale, B is 0.4 mm in length), respectively. Specimens are characteristic of Biozone 1. Modified from Godwin (2018).


Figure 27. SEM image (B) and macrophotographs (A&C) of *Taphrognathus varians* (A&B) and *Cavusgnathus unicornis* (C). *Taphrognathus varians* (A) recovered from the Barnes Unit D-2 at a depth of 8424-8424.4 ft; specimen not to scale, but 0.25 mm in lenght; (B) recovered from the Moccasin Bend Formation, Boone Group, Ottawa County, OK. *Cavusgnathus unicornis* (C) recovered from the Barnes Unit D-2 at a depth of 8424-8424.4 ft. specimen not to scale, but 0.2 mm in length. Specimens interpreted to represent Biozone 2 due to the co-occurrence of *Taphrognathus* and *Cavusgnathus* (Godwin, 2017). Image modified from Godwin (2018).

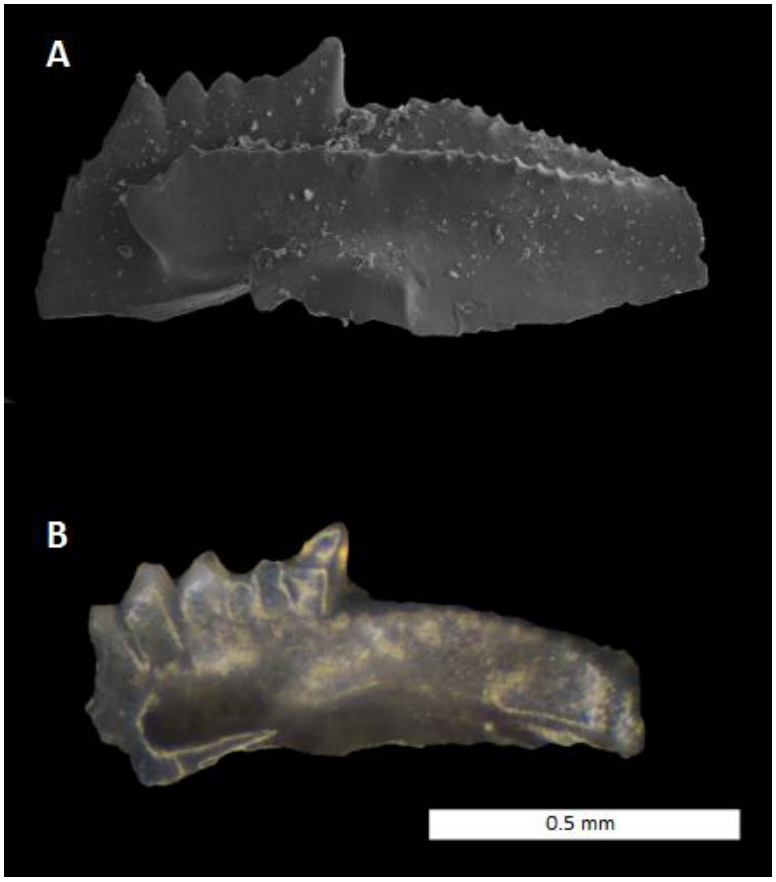


Figure 28. SEM image (A) and macrophotograph (B) of *Cavusgnathus unicornis*, recovered from the Ordnance Plant Member, Pryor Creek Formation, Mayes Group, Mayes County, OK (image shown at 60x magnification) and from the Barnes Unit D-2 at a depth of 8265.5-8266 ft (specimen B not to scale, but 0.2 mm in length), respectively. Specimens interpreted as representing Biozone 3 due to the recovery of *Cavusgnathus* without *Taphrognathus* (Godwin, 2017). Image modified from Godwin (2018).


Figure 29. SEM image (A) and macrophotograph (B) of *Gnathodus bilineatus* recovered from (A) the Hindsville Formation, Mayes Group, Washington County, AR and (B) from the Barnes Unit D-2 at a depth of 8207.6-8208.2 ft (specimen B not to scale, but 0.3 mm in length). Specimens are interpreted to represent Biozone 4 and definitively Chesterian.

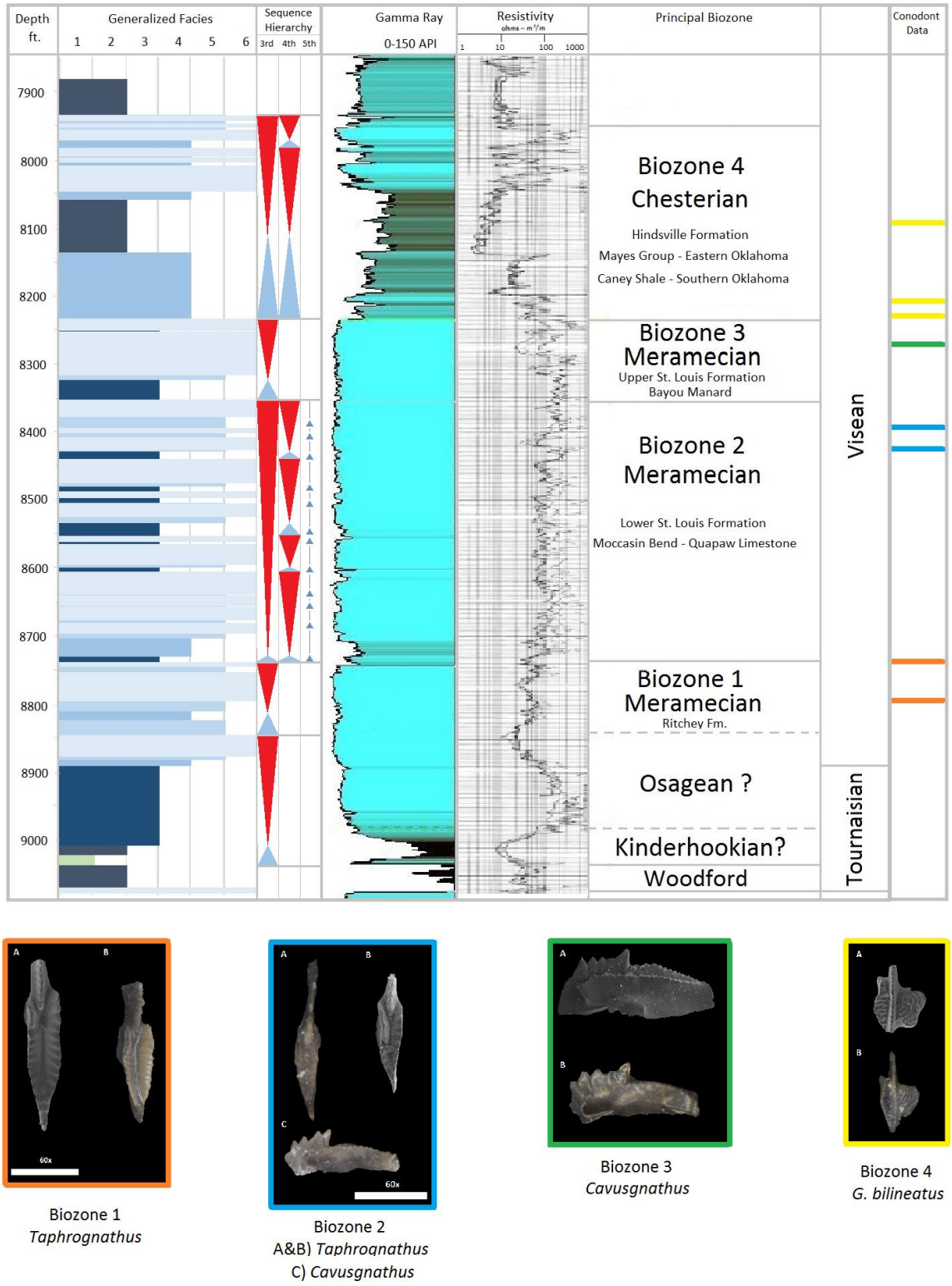


Figure 30. Summary of conodont biostratigraphic results in the Barnes D-2 core.

## Mississippian Stratigraphic Architecture

Gamma-ray wireline logs from 30 selected wells were used to construct a cross section that illustrates the Mississippian stratigraphic architecture subparallel to paleodip. The cross section spans approximately 50 miles, beginning with the Pan-American Barnes D-2 in Section 23, T. 22N., R.16W., Major County and terminates with the Pan American, Effie B. York well in Section 13, T.18N., R.09W., northwestern Kingfisher County. The Effie B. York well was selected based on the sequence stratigraphic work of Flinton (2016), available conodont biostratigraphic data (Godwin, 2018), and its geographic location within the core STACK play. Correlation of the Barnes D-2 and the Effie B. York allows interpolation across the study area and between wells with sequence stratigraphic and biostratigraphic control (Figure 31). The stratigraphic architecture of the Mississippian across the study area displays a clinoform geometry, consistent with the work of others (LeBlanc, 2014; Price, 2014; Flinton, 2016; Jaeckel, 2016). Probable 3$^{rd}$ order progradational carbonate and siliciclastic wedges are observed, resulting from an overall upward decline in sea-level across the Mississippian interval.

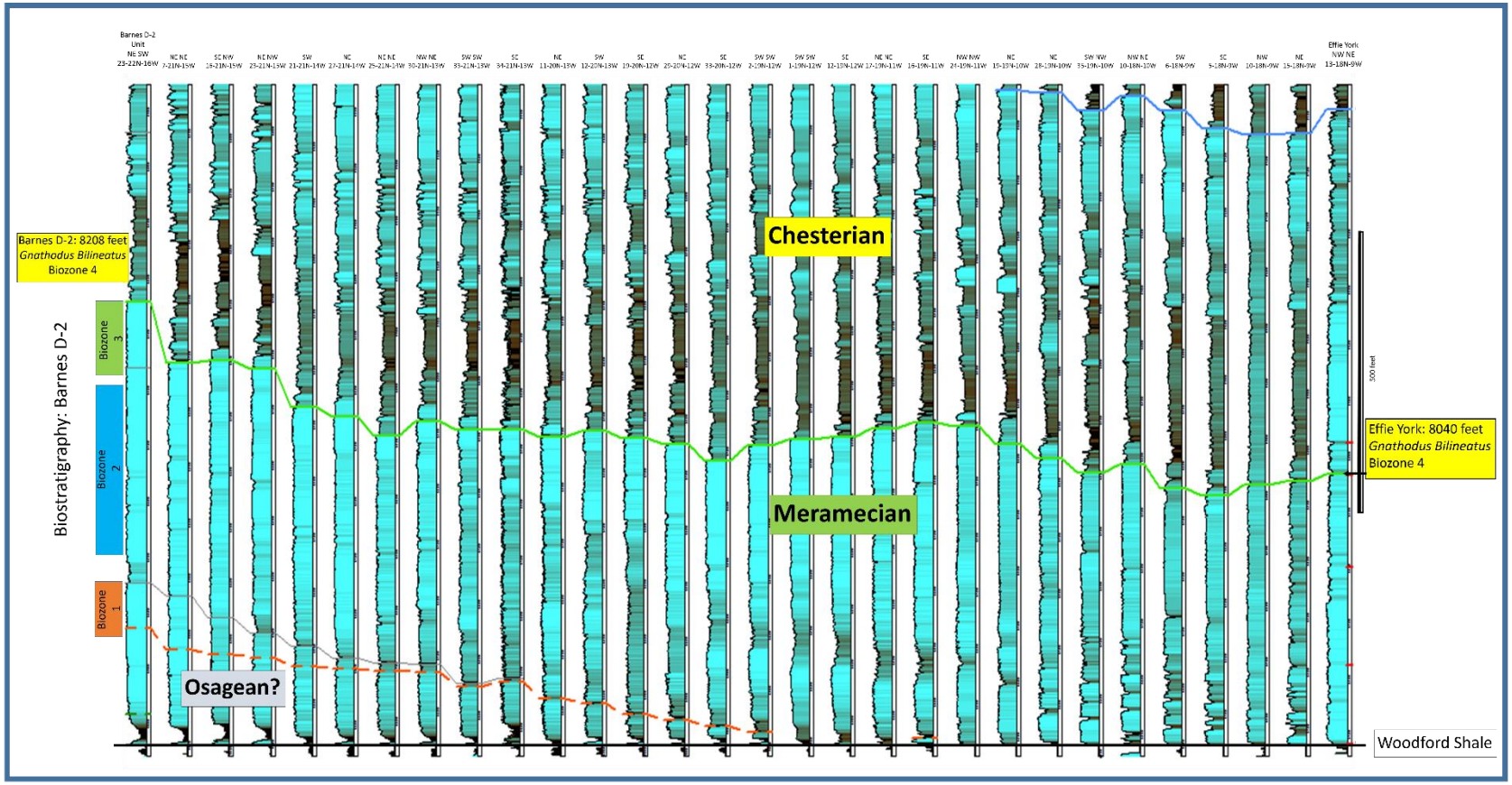


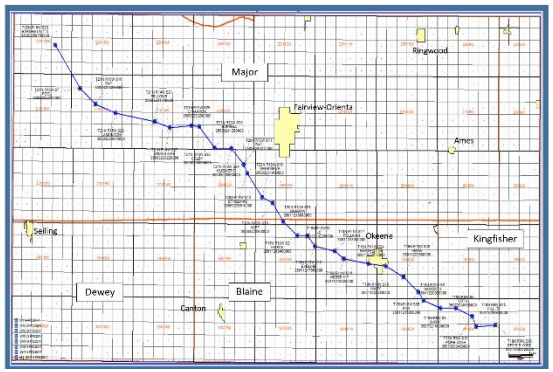


**Conclusions**

- Conodonts in the Barnes D-2 core are the same as those identified from the outcrop.
- Four principal conodont biozones
  - Biozone 4 = Chesterian
  - Biozone 3 = Meramecian
  - Biozone 2 = Meramecian
  - Biozone 1 = Meramecian
- The Meramecian-Osagean boundary has not been resolved by conodonts.
- Based on the correlation from the Barnes D-2 well in Major County, Sec. 23, T. 22N., R. 16W., to the Effie B. York well in NW Kingfisher County, Sec. 13, T. 18N., R. 9W., the "Miss Lime" section below the "Chester Shale" is Meramecian, whereas the top of Osagean is not determined with confidence.

Figure 31. Mississippian Stratigraphic Architecture. Thirty (30) selected gamma-ray wireline logs were used to construct a cross section that illustrates the Mississippian stratigraphic architecture subparallel to paleodip. This cross section begins in Major County with the Pan American, Barnes D-2 in Section 23, T. 22N., R.16W., and terminates with the Pan American, Effie B. York well in Section 13, T.18N., R.09W., northwestern Kingfisher County. The green line marks the interpreted Meramecian-Chesterian boundary and is interpolated between the Barnes D-2 and Effie B. York, both of which are partially constrained by conodont biostratigraphy. *Gnathodus bilineatus* recovered from the Effie B. York was identified by Godwin (2018).

# CHAPTER VII

## SUMMARY AND CONCLUSIONS

This study integrated conodont biostratigraphic control and sequence stratigraphic correlations to provide age constraint of Mississippian intervals within the STACK play. Correlation across the study area, between the Barnes D-2 in western Major County, OK and the Effie B. York in northwestern Kingfisher County, OK illustrates the stratigraphic architecture of the Mississippian Subsystem. The key findings including specific ones supporting the initial hypothesis that the cored interval in the Barnes D-2 is Meramecian Age and that this biostratigraphic framework can be correlated into the STACK play, as follows:

1. Core and thin-section analyses reveal six generalized depositional facies within the Barnes D-2 core.
2. Analyses of these facies and their vertical stacking patterns suggest a hierarchy of four depositional sequences and cycles. The gross Mississippian interval within the study area is interpreted to represent a 2$^{nd}$ order, overall shallowing-upward supersequence. Three levels of depositional cyclicity are demonstrated within this 2$^{nd}$ order supersequence (3$^{rd}$, 4$^{th}$, and 5$^{th}$ order). Five 3$^{rd}$ order depositional sequences (S1-S5) were recognized in the Barnes D-2 core. High frequency sequences (4$^{th}$ order) and cycles (5$^{th}$ order) were variably recognized within these 3$^{rd}$ order sequences.
3. The 3$^{rd}$ order depositional sequences identified in the Barnes D-2 core (S2-S5)

were constrained by conodont biostratigraphy, providing ages for Mississippian intervals in the STACK play through subsequent correlation.

4. The Mississippian interval (S2-S5) in the Barnes D-2 core from oldest to youngest are Biozone 1 (early Meramecian – Ritchey Formation in outcrop), Biozone 2 (middle Meramecian – lower St. Louis in outcrop), Biozone 3 (upper Meramecian – upper St. Louis in outcrop) and Biozone 4 (Chesterian – Hindsville Formation in outcrop).
5. The contact between the Meramecian and Chesterian was identified honoring biostratigraphic constraints.
6. The Meramecian-Osagean boundary could not be resolved due to limited conodont recovery. However, Osagean rocks may still be present in the approximately 200 ft of Mississippian carbonate section below the first identified biozone.
7. The Mississippian interval commonly referred to as "Meramecian-Osagean," or "Osagean" is actually Meramecian.
8. The Mississippian stratigraphic architecture in the study area displays a clinoform geometry consisting of progradational mixed carbonate-siliciclastic sequences, characteristic of a distally-steepened ramp environment.
9. Integration of biostratigraphic and sequence stratigraphic analyses in the Barnes D-2 reveals the relatively high frequency $4^{th}$ and $5^{th}$ order cyclicity observed in the "S3" $3^{rd}$ order sequence (Biozone 2) corresponds with the middle Meramecian, which is important as Flinton (2016) and Jaeckel (2016) point out

that high frequency cyclicity can impart controls on reservoir development and vertical compartmentalization.

# REFERENCES


Asquith, G. and Krygowski, D., 2004, Basic Well Log Analysis, 2nd Edition, AAPG Methods in Exploration Series, No. 16, 244 p.

Ausich, W.I., Kammer, T.W., and Baumiller, T.K., 1994, Demise of the Middle Paleozoic crinoid fauna–a single extinction event or rapid faunal turnover?: Paleobiology, v. 20, p. 345-361.

Bahrami, A., Boncheva, I., Konigshof, P., Yazdi, M., and Ebrahimi Khan-Abadi, A., 2014, Conodonts of the Mississippian/Pennsylvanian boundary interval in central Iran: Journal of Asian Earth Sciences, v. 92, p. 187-200.

Baesemann, J.F. and Lane, H.R., 1985, Taxonomy of the genus *Rhachistognathus* Dunn (Conodonta–Late Mississippian to Early Pennsylvanian), *in* Lane, H.R. and Ziegler, W., eds., Toward a Boundary in the Middle of the Carboniferous–Stratigraphy and Paleontology: Courier Forschungsinstitut Senckenberg 74, p. 93-115.

Batt, L.S., Montanez, I.P., Isaacson, P., Pope, M.C., Butts, S.H., Abplanalp, J., 2007, Multi-carbonate component reconstruction of mid-Carboniferous (Chesterian) 107 seawater $\delta$13C: Paleogeography, Paleoclimatology, Paleoecology, v. 256, p. 298-318, doi: 10.1016/j.palaeo.2007.02.049.

Bertalott, J.R., 2014, Core- and log-based stratigraphic framework of Mississippian limestone in portions of north-central Oklahoma [M.S. Thesis]: Stillwater, Oklahoma State University, 144 p.

Blakey, R., 2018, North American key time slices: Deep Time Maps, http://deeptimemaps.com/wp-content/uploads/2016/05/NAM_key-345Ma_EMiss.png (accessed November 2018).

Boardman, D.R., Mazzullo, S.J., Wilhite, B.W., Puckette, J.O., Thompson, T.L., and Woolsey, I.W., 2010, Diachronous prograding carbonate wedges from the burlington shelf to the southern distal shelf/basin in the southern flanks of the Ozarks, Abstracts with Programs, North-Central and South-Central Section Meeting, Geological Society of America, v. 42, no. 2, p.41.

Boardman, D.R., Thompson, T.L., Godwin, C.J., Mazzullo, S.J., Wilhite, B.W., and Morris, B.T., 2013, High-resolution conodont zonation for Kinderhookian (middle Tournaisian) and Osagean (upper Tournaisian-lower Visean) strata of the western edge of the Ozark Plateau, North America: Oklahoma City Geological Society Shale Shaker, v. 64, p. 98-151.

Briggs, D.E.G., Clarkson, E.N.K., and Aldridge, R.J., 1983, The conodont animal: Lethaia, v. 16, p. 1-14, doi:10.1111/j.1502-3931.1983.tb01993.x.

Buggisch, W., Joachimski, M. M., Sevastopulo, G., and Morrow, J. R., 2008, Mississippian $\delta^{13}C_{carb}$ and conodont apatite $\delta^{18}O$ records – their relation to the Late Palaeozoic glaciation: palaeogeography, palaeoclimatology, palaeoecology 268, p. 273-292.

Burchette, T.P. and Wright, V.P., 1992, Carbonate ramp depositional systems: Sedimentary Geology, v. 79, p. 3-57.

Childress, M.N., 2015, High-resolution sequence stratigraphic architecture of a Mid-Continent Mississippian outcrop in southwest Missouri [M.S. Thesis]: Stillwater, Oklahoma State University, 272 p.

Childress, M. and Grammer, G.M., 2015, High resolution sequence stratigraphic architecture of a Mid-Continent Mississippian outcrop in southwest Missouri, Shale Shaker, v. 66, no. 4, p. 206-234.

Choquette, P. W., and Pray, L. C., 1970, Geologic Nomenclature and Classification of Porosity in Sedimentary Carbonates, AAPG Bulletin, v. 54, no. 2, p. 207-250.

Collinson, C., Rexroad, C.B., and Thompson, T.L., 1970, Conodont zonation of the North American Mississippian: Geological Society of America Memoir 127, p. 353-394, doi: 10.1130/MEM127-p353.

Curtis, D. M. and Champlin, S. C., 1959, Depositional environments of Mississippian limestones of Oklahoma, Tulsa Geological Society Digest, v. 27, no. 1, p. 90-103.

Doll, P.L., 2015, Determining structural influence on depositional sequences in carbonates using core-calibrated wireline logs–Mississippian aged carbonates, Mid-Continent, USA [M.S. Thesis]: Stillwater, Oklahoma State University, 167 p.

Dunham, R.J., 1962, Classification of carbonate rocks according to depositional texture, AAPG Special Volumes, Memoir 1: Classification of Carbonate Rocks, v. 1, p. 108-121.

Dunn, D.L., 1970, Middle Carboniferous conodonts from western United States and phylogeny of the platform group: Journal of Paleontology, v. 44, p. 312-342.

Dupont, A.M., 2016, High-resolution chemostratigraphy in the "Mississippian Limestone" of north-central Oklahoma [M.S. Thesis]: Stillwater, Oklahoma State University, 147 p.

Ekdale, A.A., Bromley, R.G., and Pemberton, S.G., 1984, Ichnology – trace fossils in sedimentology and stratigraphy, SEPM Short Course No. 15, 317 p.

Evans, K. R., Jackson, J. S., Mickus, K. L., Miller, J. F., and Cruz, D., 2011, Enigmas and anomalies of the Lower Mississippian Subsystem in outhwestern Missouri, Search and Discovery Article #50406, 47 p.

Flinton, K.C., 2016, The effects of high-frequency cyclicity on reservoir characteristics of the "Mississippian Limestone", Anadarko Basin, Kingfisher County, Oklahoma [M.S. Thesis]: Stillwater, Oklahoma State University, 414 p.

Franseen, E.K., 2006, Mississippian (Osagean) Shallow-water, mid-latitude siliceous sponge spicule and heterozoan carbonate facies: an example from Kansas with implications for regional controls and distribution of potential reservoir facies, Current Research in Earth Sciences, Bulletin 252, pg. 1-23.

Godwin, C.J., 2017, Lithostratigraphy and conodont biostratigraphy of the upper Boone Group and Mayes Group in the southwestern Ozarks of Oklahoma, Missouri, Kansas, and Arkansas [Ph.D. Dissertation]: Stillwater, Oklahoma State University, 402 p.

Godwin, C.J., 2018, Outcrop-based conodont biostratigraphy of the Meramecian through middle Chesterian (Viséan) rocks of northeastern Oklahoma and their preliminary correlation into the subsurface, Paper presented at the Oklahoma Geological Survey STACK Play Workshop, Oklahoma City, OK.

Gradstein, F.M., Ogg, J.G., and Ogg, G.M., eds., 2012, A concise geologic time scale: Elsevier, p. 99-113, doi: 10.1016/B978-0-444-59467-9.00009-1.

Gunnell, F.H., 1931, Conodonts from the Fort Scott Limestone of Missouri: Journal of Paleontology, v. 5, p. 244–252.

Gutschick, R., and Sandberg, C.A., 1983, Mississippian continental margins of the conterminous United States, SEPM Special Publication, N. 33, p. 79-96.

Handford, C. R., 1986, Facies and bedding sequences in shelf-storm-deposited carbonates – Fayetteville Shale and Pitkin Limestone (Mississippian), Arkansas, Journal of Sedimentary Petrology, v. 56, no. 1, p. 123-137.

Handford, C.R., 1995, Baselap patterns and the recognition of lowstand exposure and drowning–a Mississippian ramp example and its seismic signature: Journal of Sedimentary Research, v. 65, p. 323-337.

Haq, B. U., and Schutter, S. R., 2008, A chronology of paleozoic sea-level changes, Science, v. 322, p. 64-68.

Hunt, J., 2017, Conodont biostratigraphy in middle Osagean to upper Chesterian strata, north-central Oklahoma, U.S.A. [M.S. Thesis]: Stillwater, Oklahoma State University, 190 p.

Jaeckel, L., 2016, High-resolution sequence stratigraphy and reservoir characterization of Mid-Continent Mississippian carbonates in north-central Oklahoma and south-central Kansas [M.S. Thesis]: Stillwater, Oklahoma State University, 368 p.

Jordan, L. and Rowland, T.L., 1959, Mississippian rocks in Northern Oklahoma, Tulsa Geological Society Digest, v. 27, p. 124-136.

Kerans, C. and Tinker, S.W., 1997, Sequence stratigraphy and characterization of carbonate reservoirs: Society of Economic Paleontologists and Mineralogists Short Course Notes No. 40, p. 1-130.

Koch, J.T., Frank, T.D., and Bulling, T.P., 2014, Stable-isotope chemostratigraphy as a tool to correlate complex Mississippian marine carbonate facies of the Anadarko shelf, Oklahoma and Kansas: American Association of Petroleum Geologists Bulletin, v. 98, p. 1071-1090, doi: 10.1306/10031313070.

Krumhardt, A.P., Harris, A.G., and Watts, K.F., 1996, Lithostratigraphy, microlithofacies, and conodont biostratigraphy and biofacies of the Wahoo Limestone (Carboniferous), eastern Sadlerochit Mountains, Northeast Brooks Range, Alaska: United States Geological Survey Professional Paper 1568, 88 p.

Lane, H.R. and Brenkle, P.L., 2005, Type Mississippian subdivisions and biostratigraphic succession, *in* Heckel, P.H., ed., Stratigraphic and biostratigraphy of the Mississippian Subsystem (Carboniferous System) in its type region, the Mississippi River valley of Illinois, Missouri, and Iowa: International Union of Geological Sciences Subcomission on Carboniferous Stratigraphy, Guidebook for Field Conference, St. Louis, Missouri, 8-13 September 2001: Champaign, Illinois, Illinois State Geological Survey Guidebook 34, p. 83-107.

Laudon, L.R., 1948, Osage-Meramec contact: The Journal of Geology, v. 56, p. 288-302.

Lane, H. R., and DeKyser, T. L., 1980, Paleogeography of the Late Early Mississippian (Tournasian 3) in the Central and Southwestern United States, Paleozoic Paleogeography of West-Central United States: Rocky Mountain Paleogeography Symposium 1, p. 149-162.

LeBlanc, S.L., 2014, High-resolution sequence stratigraphy and reservoir characterization of the "Mississippian Limestone" in north-central Oklahoma [M.S. Thesis]: Stillwater, Oklahoma State University, 443 p.

Maples, C.G. and J.A. Waters, 1987, Redefinition of the Meramecian/Chesterian boundary (Mississippian): Geology, v. 15, p. 647-651.

Mazzullo, S.J., 2011, Mississippian Oil Reservoirs in the Southern Midcontinent: New Exploration Concepts for a Mature Reservoir Objective, AAPG Search and Discovery, Article no. 10373, November, p. 1-34.

Mazzullo, S.J., Boardman, D. R., Wilhite, B. W., Godwin, C. J., and Morris, B. T., 2013, Revisions of outcrop lithostratigraphic nomenclature in the Lower to Middle Mississippian Subsystem (Kinderhookian to Basal Meramecian Series) along the shelf-edge in southwest Missouri, northwest Arkansas, and northeast Oklahoma, Shale Shaker, v. 63, no. 6, p. 414-454.

Mazzullo, S.J., and Wilhite, B. W., 2010, Chert, tripolite, spiculite, Chat – What's in a name?, Kansas Geological Society Bulletin, v. 85, no. 1, p. 21-25.

Mazzullo, S.J., Wilhite, B.W., and Boardman, D.R., 2011a, Lithostratigraphic architecture of the Mississippian Reeds Spring Formation (middle Osagean) in southwest Missouri, northwest Arkansas, and northeast Oklahoma–outcrop analog of subsurface petroleum reservoirs: Oklahoma City Geological Society Shale Shaker, v. 61, p. 254-269.

Mazzullo, S.J., Wilhite, B. W., Boardman, D. R., Morris, B., Turner, R., and Godwin, C., 2011b, Field Trip Guidebook: Lithostratigraphy and conodont biostratigraphy of

the Kinderhookian to Osagean series on the western flank of the Ozark Uplift, Sponsored by the Tulsa Geological Society, 48 p.

Mazzullo, S.J., Wilhite, B. W., and Woolsey, I. W., 2009a, Rhythmic carbonate versus spiculite deposition in Mississippian hydrocarbon reservoirs in the Midcontinent USA: causative factors and resulting reservoir petrophysical attributes, AAPG Search and Discovery Article #10209, 6 p.

Mazzullo, S.J., Wilhite, B. W., and Woolsey, I. W., 2009b, Petroleum reservoirs within a spiculite-dominated depositional sequence: Cowley Formation (Mississippian: Lower Carboniferous), south-central Kansas, AAPG Bulletin, v. 93, no. 12, p. 1649-1689.

Miall, A.D., 2013, The geology of stratigraphic sequences: New York, Springer-Verlag Berlin Heidelberg, 435 p.

Middleton, G. V., Church, M. J., Coniglio, M., Hardie, L. A., and Longstaffe, F. J., 2003, Encyclopedia of sediments and sedimentary rocks, Kluwer Academic Publishers, The Netherlands, 821 p.

Mii, H., Grossman, E.L., and Yancey, T.E., 1999, Carboniferous isotope stratigraphies of North America–implications for Carboniferous paleoceanography and Mississippian glaciation: Geological Society of America Bulletin, v. 111, p. 960-973.

Miller, J.D., 2015, Conodont biostratigraphy of the upper Osagean (lower Visean) Ozark Uplift, southern Midcontinent, USA [M.S. Thesis]: Stillwater, Oklahoma State University, 149 p.

Morrow, J.R. and Webster, G.D., 1991, Carbonate microfacies and related conodont biofacies, Mississippian-Pennsylvanian boundary strata, Granite Mountain, west-central Utah, *in* Kowallis, B.J. and Seely, K., eds., Brigham Young University Geology Studies v. 37: Department of Geology, Brigham Young University, p. 99-124.

Noble, P.J., 1993, Paleoceanographic and tectonic implications of a regionally extensive Early Mississippian hiatus in the Ouachita system, southern mid-continental United States: Geology, v. 21, p. 315-318.

Northcutt, R. A., and Campbell, J. A., 1996, Geologic provinces of Oklahoma, Transactions of the 1995 AAPG Mid-Continent Section Meeting, 1996, p. 128-134.

Pander, C.H., 1856, Monographie der fossilen Fische der Silurischen systems der Russisch Baltischen Gouvernements: Obersilurische Fische, Buchdruckerei Kaiserlichen Akademie des Wissenschaften, St. Petersburg, 91 p.

Perri, M.C. and Spaletta, C., 1998, Conodont distribution at the Tournaisian/Visean boundary in the Carnic Alps (Southern Alps, Italy), *in* Szaniawski, H., ed., 124 Proceedings of the Sixth European Conodont Symposium: Paleontologica Polonica, v. 58, p. 225-245.

Price, B.J., 2014, High-resolution sequence stratigraphic architecture and reservoir characterization of the Mississippian Burlington/Keokuk Formation, northwestern Arkansas [M.S. Thesis]: Stillwater, Oklahoma State University, 144 p.

Read, J.F., 1985, Carbonate platform facies models: American Association of Petroleum Geologists Bulletin, v. 69, p. 1-21.

Ross, C.A. and Ross, J.R.P., 1987a, Biostratigraphic zonation of Late Paleozoic depositional sequences, *in* Ross, C.A. and Haman, D., eds., Timing and depositional history of eustatic sequences–constraints on seismic stratigraphy: Cushman Foundation for Foraminiferal Research, Special Publication 24, p. 151-168.

Ross, C.A. and Ross, J.R.P., 1987b, Late Paleozoic sea levels and depositional sequences, *in* Ross, C.A. and Haman, D., eds., timing and depositional history of eustatic sequences–constraints on seismic stratigraphy: Cushman Foundation for Foraminiferal Research Special Publication 24, p. 137-150.

Roundy, P.V., 1926, The microfauna of Mississippian formations of San Saba County, Texas: United States Geological Survey Professional Paper 146, p. 5–17.

Russell, M.P., 2013, Echinoderm responses to variation in salinity: Advances in Marine Biology, v. 66, p. 171-212.

Saltzman, M.R., 2002, Carbon and oxygen isotope stratigraphy of the Lower Mississippian (Kinderhookian to lower Osagean), western United States–implications for seawater chemistry and glaciation: Geological Society of America Bulletin, v. 114, p. 96-108.

Saltzman, M.R., 2003, Late Paleozoic ice age–Oceanic gateway or pCO2?: Geology, v. 31, p.151-154.

Scholle, P.A., and Ulmer-Scholle, D.S., 2003, A color guide to the petrography of carbonate rocks: grains, textures, porosity, diagenesis, AAPG Memoir 77, Tulsa, The American Association of Petroleum Geologists, 474 p.

Shelley, S.A., 2016, Outcrop-based sequence stratigraphy and reservoir characterization of an Upper Mississippian mixed carbonate-siliciclastic ramp, Mayes County, Oklahoma [M.S. Thesis]: Stillwater, Oklahoma State University, 92 p.

Sloss, L. L., 1963, Sequences in the cratonic interior of North America, Geological Society of America Bulletin 74, p. 93-114.

Snedden, J.W. and Liu, C., 2010, A compilation of Phanerozoic sea-level change, coastal onlaps and recommended sequence designations: American Association of Petroleum Geologists Search and Discovery Article #40594, 3 p.

Snedden, J.W. and Liu, C., 2011, Recommendations for a uniform chronostratigraphic desgination system for Phanerozoic depositional sequences: American Association of Petroleum Geologists Bulletin, v. 95, p. 1095-1122.

Stauffer, C. R., 1930, Conodonts from Decorah shale: Journal of Paleontology, v. 4, no. 2, p. 121-128.

Stauffer, C. R., & Plummer, H. J., 1932, Texas Pennsylvanian conodonts and their stratigraphic relations: University of Texas Bulletin, p. 13-50.

Sweet, W.C. and Cooper, B.J., 2008, C.H. Pander's introduction to conodonts, 1856: Episodes, v. 31, p. 429-432.

Taylor, A. M., & Goldring, R., 1993, Description and analysis of bioturbation and ichnofabric: Journal of the Geological Society, v. 150(1), p. 141-148, doi: 10.1144/gsjgs.150.1.0141

Thompson, T.L., and Fellows, L.D., 1970, Stratigraphy and conodont biostratigraphy of Kinderhookian and Osagean (Lower Mississippian) rocks of southwestern

Missouri and adjacent areas, Missouri Geological Survey and Water Resources Report of Investigations 45, 263 p.

Ulrich, E.O. and Bassler, R.S., 1926, A classification of the toothlike fossils, conodonts, with descriptions of American Devonian and Mississippian species: Proceedings of the United States National Museum, v. 68, p.1-63.

Zeller, D.E., ed., 1968, Stratigraphic succession in Kansas: Geological Survey Bulletin 189, http://www.kgs.ku.edu/Publications/Bulletins/189/index.html (accessed March 2019).

# APPENDICES

## APPENDIX A: CONODONT PLATES

All SEM images scaled to 60x, white scale bar is 0.5 mm. Macrophotograph specimens not to scale, but lengths are reported in respective lists below. All specimens held at the Paleontology Repository, Department of Earth and Environmental Sciences, University of Iowa. Plates prepared by Cory Godwin (2018), Ph.D. Oklahoma State University.

**PLATE 1 – Biozone 1**

Figure A – *Gnathodus pseudosemiglaber* (Thompson and Fellows); Bentonville Formation, Boone Group; Ottawa County, OK.

Figure B – *Gnathodus pseudosemiglaber* (Thompson and Fellows); Tahlequah Limestone, Boone Group; Cherokee County, OK; SUI 141191.

Figure C –*Taphrognathus varians* Branson and Mehl; Ritchey Formation, Boone Group; Ottawa County, OK; SUI 141687.

Figure D – *Lochriea homopunctatus* (Ziegler); Tahlequah Limestone, Boone Group; Cherokee County, OK; SUI 141560.

Figure E – *Taphrognathus varians* Branson and Mehl. Barnes Unit D #2; Major County, OK; Depth: 8786.4-8786.9 feet; Length: 0.4 mm; SUI 109275.

Figure F – *Gnathodus pseudosemiglaber* (Thompson and Fellows); Barnes Unit D #2; Major County, OK; Depth: 8741.3 feet; Length: 0.2 mm; SUI 109628.

Figure G – *Gnathodus* n. sp. 15 (aff. *punctatus*) Boardman et al. (2013); Ritchey Formation, Boone Group; Ottawa County, OK; SUI 141679.

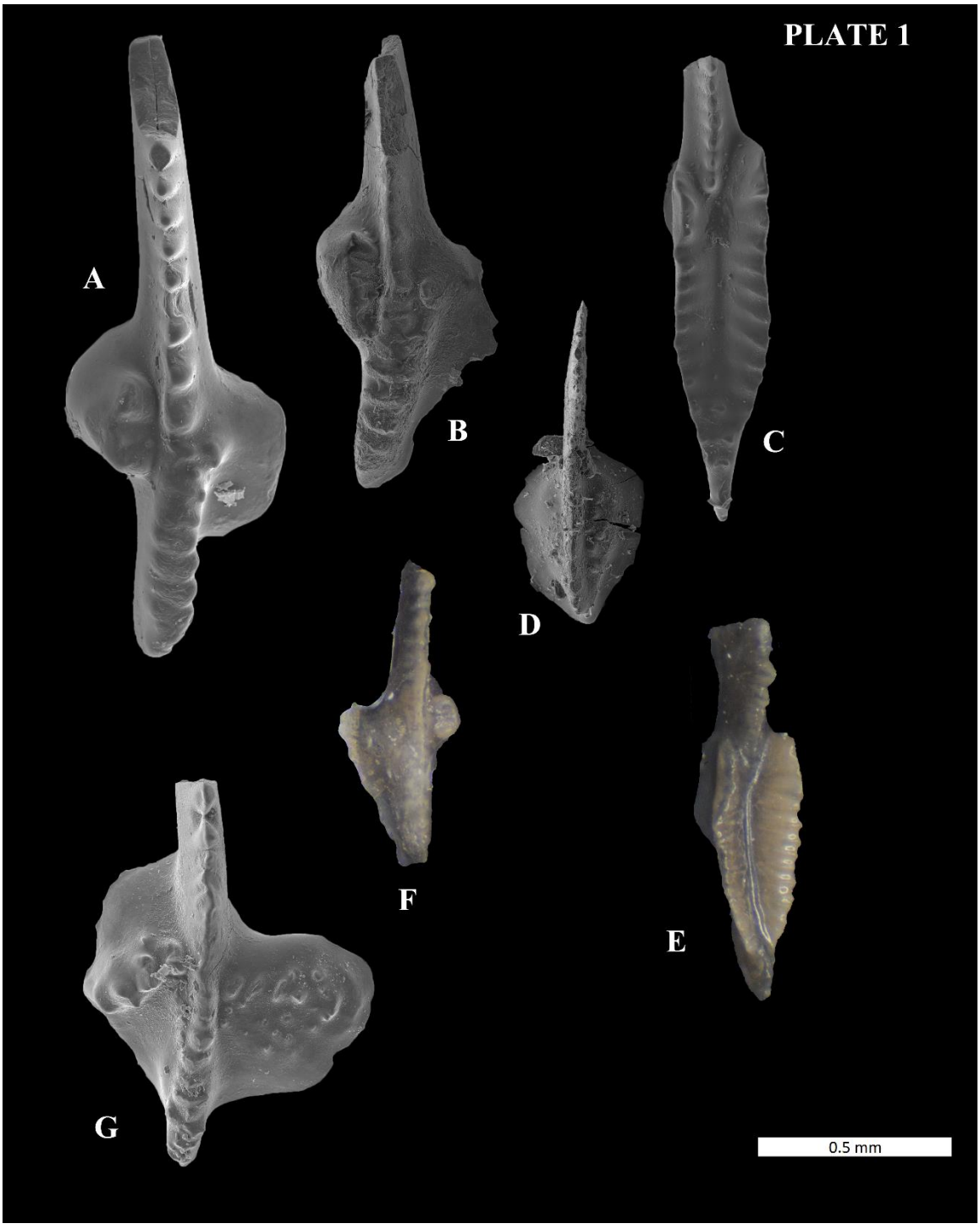
PLATE 1
A
B
C
D
E
F
G
0.5 mm

**PLATE 2 – Biozone 2**

Figure A – *Taphrognathus varians* Branson and Mehl; Barnes Unit D #2; County, OK; Depth: 8424-8424.4 ft; Length: 0.25 mm; SUI 109559.

Figure B – *Taphrognathus varians* Branson and Mehl; Moccasin Bend Formation, Boone Group; Ottawa County, OK; SUI 141234.

Figure C – *Hindeodus cristula* (Youngquist and Miller, 1949); Moccasin Bend Formation, Boone Group; Craig County, OK); SUI 141458.

Figure D – *Cavusgnathus altus* (Harris and Hollingsworth); Moccasin Bend Formation, Boone Group; Craig County, OK; SUI 141219.

Figure E – *Cavusgnathus unicornis* (Youngquist and Miller); Barnes Unit D #2; Major County, OK; Depth: 8424-8424.4 ft; Length: 0.2 mm; SUI 109660.

Figure F – *Lochriea homopunctatus* (Ziegler); Barnes Unit D #2; Major County, OK; Depth: 8395.1-8395.6 feet; Length: 0.15 mm; SUI 109654.

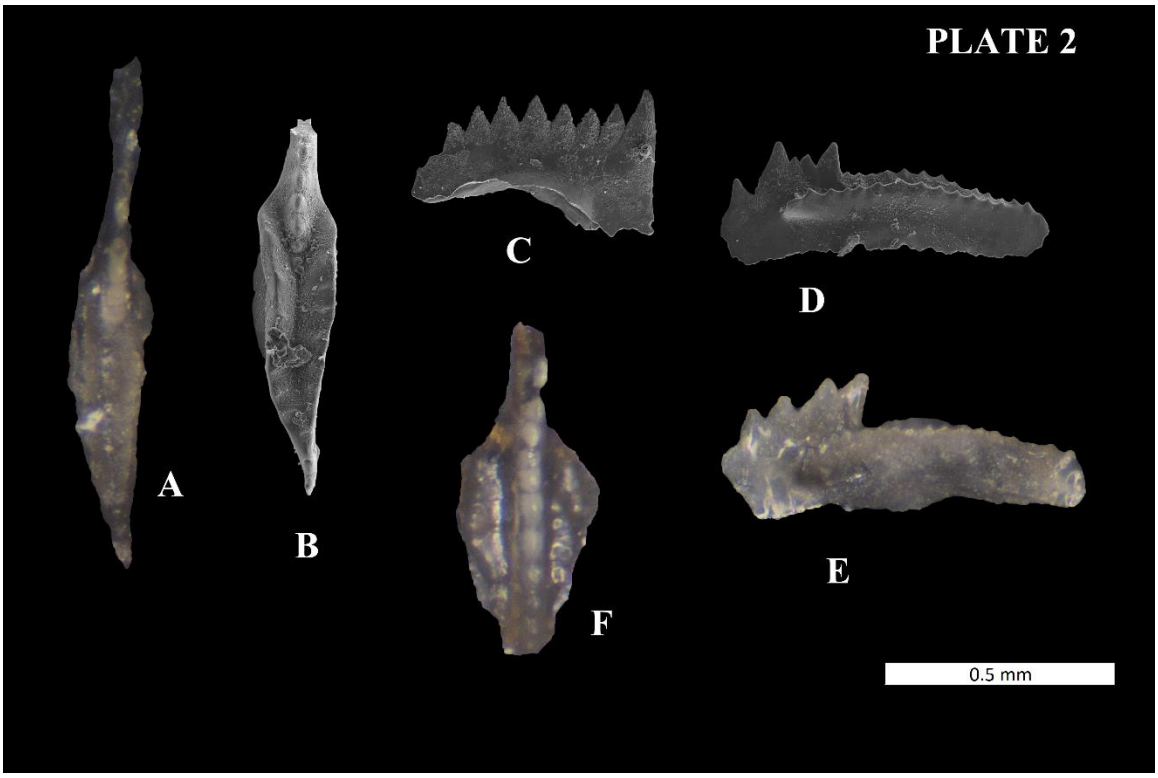
PLATE 2
A
B
C
D
E
F
0.5 mm

**PLATE 3 – Biozone 3**

Figure A – *Hindeodus cristula* (Youngquist and Miller, 1949); Ordnance Plant Member, Pryor Creek Formation, Mayes Group; Mayes County, OK; SUI 141631.

Figure B – *Hindeodontoides spiculus* (Youngquist and Miller, 1949); Ordnance Plant Member, Pryor Creek Formation, Mayes Group; Mayes County, OK; SUI 141633.

Figure C – *Hindeodus cristula* (Youngquist and Miller, 1949); Barnes Unit D #2; Major County, OK; Depth: 8237.8-8238.5 feet; Length: 0.16 mm; SUI 109286.

Figure D – *Cavusgnathus unicornis* (Youngquist and Miller); Ordnance Plant Member, Pryor Creek Formation, Mayes Group; Mayes County, OK; SUI 141275.

Figure E – *Cavusgnathus unicornis* (Youngquist and Miller); Barnes Unit D #2; Major County, OK; Depth: 8265.5-8266 feet; Length: 0.2 mm; SUI 109292.

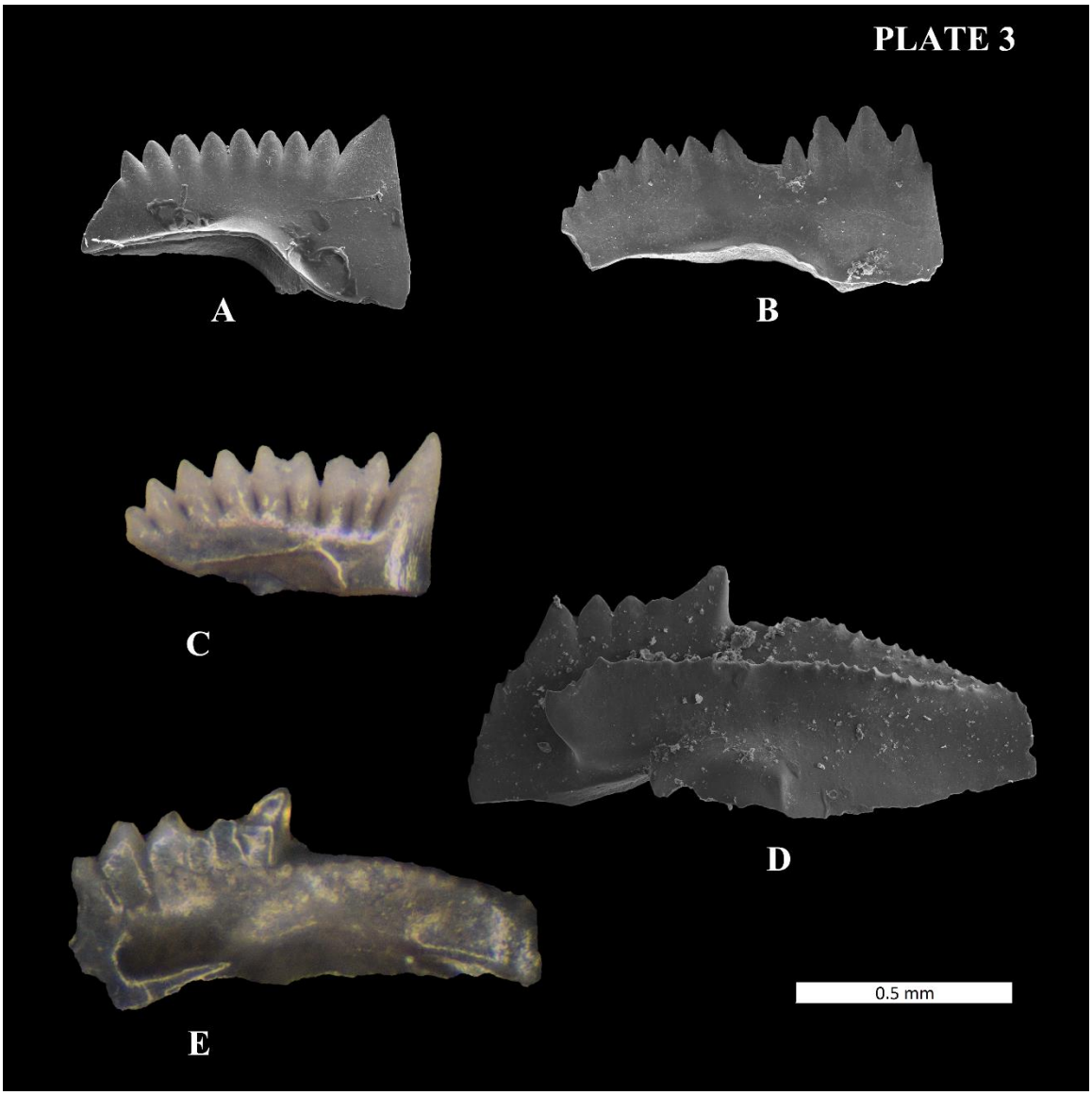
PLATE 3
A
B
C
D
E
0.5 mm

**PLATE 4 – Biozone 4**

Figure A – *Gnathodus bilineatus* (Roundy); Ordnance Plant Member, Pryor Creek Formation; Mayes County, OK; SUI 141264.

Figure B – *Gnathodus bilineatus* (Roundy); Hindsville Formation, Mayes Group; Washington County, AR; SUI 141311.

Figure C – *Lochriea commutata* (Branson and Mehl); Lindsey Bridge Member, Pryor Creek Formation, Mayes Group; Mayes County, OK; SUI 141252.

Figure D – *Lochriea commutata* (Branson and Mehl); Hindsville Formation, Mayes Group; Mayes County, OK; SUI 141288.

Figure E – *Rhachistognathus* sp. B; Lindsey Bridge Member, Pryor Creek Formation, Mayes Group; Mayes County, OK SUI 141624.

Figure F – *Gnathodus girtyi girtyi* (Hass); Lindsey Bridge Member, Pryor Creek Formation, Mayes Group; Mayes County, OK; SUI 141621.

Figure G – *Gnathodus girtyi girtyi* (Hass); Lindsey Bridge Member, Pryor Creek Formation, Mayes Group; Mayes County, OK; SUI 141249.

Figure H – *Gnathodus girtyi girtyi* (Hass); Lindsey Bridge Member, Pryor Creek Formation, Mayes Group; Mayes County, OK; SUI 141260.

Figure I – *Gnathodus bilineatus* (Roundy); Barnes Unit D #2; Major County, OK; Depth: 8207.6-8208.2 ft; Length: 0.3 mm; SUI 109280.

Figure J – *Cavusgnathus regularis* (Youngquist and Miller); Barnes Unit D #2; Major County, OK, Depth: 8093-8093.8 feet; Length: 0.5 mm; SUI 109615.

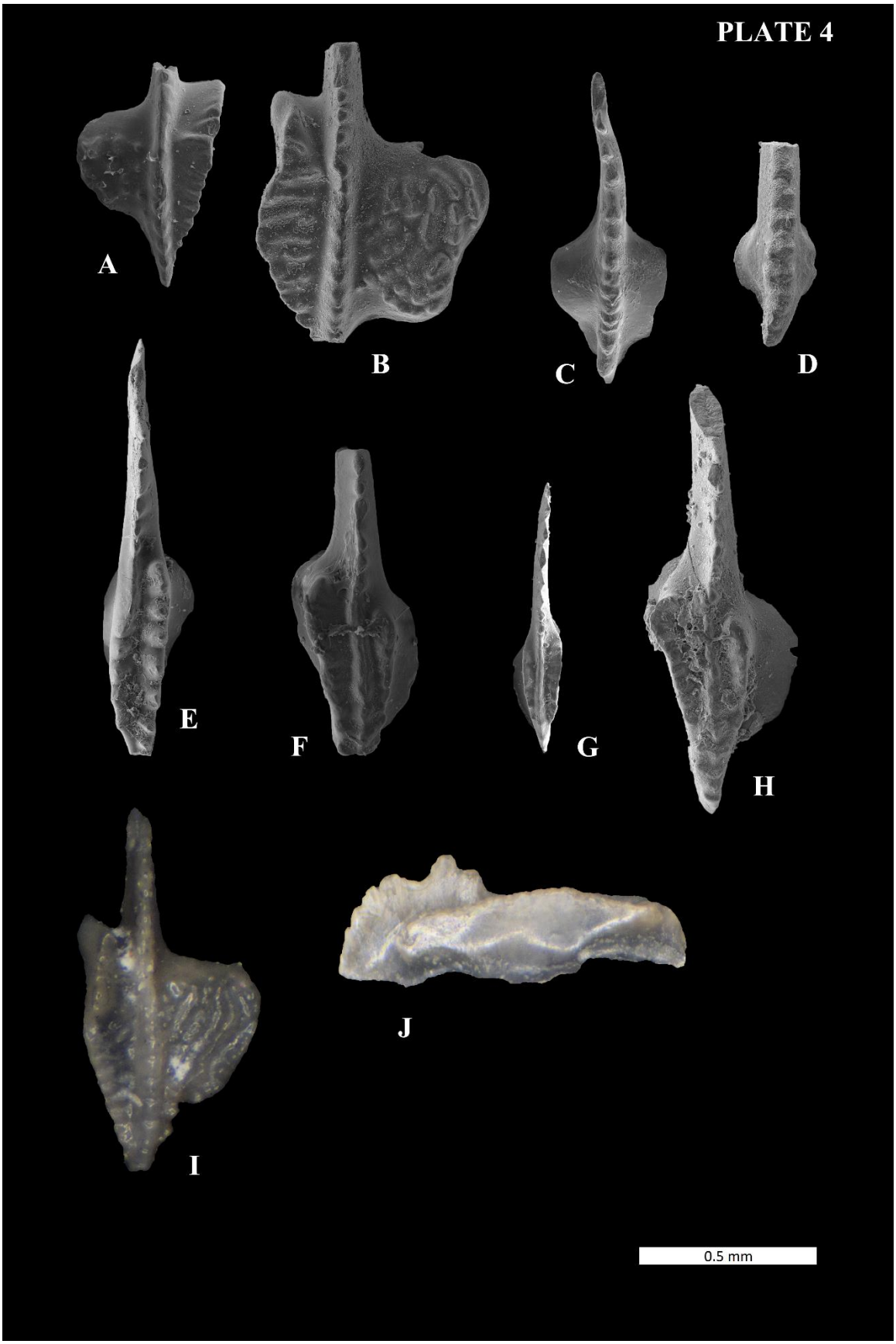
PLATE 4
A
B
C
D
E
F
G
H
I
J
0.5 mm

VITA

Brandon Chase Stukey

Candidate for the Degree of

Master of Science

Thesis: BIOSTRATIGRAPHICALLY CONSTRAINED AGES OF MISSISSIPPIAN MIXED CARBONATE-SILICICLASTIC SEQUENCES, STACK PLAY, ANADARKO BASIN, OKLAHOMA

Major Field: Geology

Biographical:

Education:

Completed the requirements for the Master of Science in Geology at Oklahoma State University, Stillwater, Oklahoma in May, 2020.

Completed the requirements for the Bachelor of Science in Nursing at University of Oklahoma Health Sciences Center, Oklahoma City, Oklahoma in July, 2012.

Completed the requirements for the Bachelor of Science in Psychology at Oklahoma State University, Stillwater, Oklahoma in May, 2006

Experience:

February 2020 to Present: Geologist, Midwest Energy Investments

Professional Memberships:

American Association of Petroleum Geologist

Oklahoma City Geological Society